

Linear mechanistic models for the dorsal lateral geniculate nucleus of cat probed using drifting-grating stimuli

G T Einevoll¹ and H E Plesser

Physics, ITF, Agricultural University of Norway, 1432 Ås, Norway

E-mail: gaute.einevoll@nlh.no

Received 22 January 2002, in final form 6 September 2002

Published 25 September 2002

Online at stacks.iop.org/Network/13/503

Abstract

Experiments with sinusoidal visual stimuli in the early visual pathway have traditionally been interpreted in terms of descriptive filter models. We present an alternative mechanistic approach for interpretation of this type of data recorded from X cells in the dorsal lateral geniculate nucleus (dLGN) of cat. A general, linear, rate-based mathematical expression for the geniculate transfer ratio, i.e. the ratio between the first-harmonic components of the output of a geniculate relay cell and its retinal input, is derived. In linear theory this ratio is independent of the signal processing occurring at the retinal level. Further, the ratio is straightforwardly accessible in experiments due to the presence of S-potentials, representing the retinal input, in extracellular recordings from dLGN. The expression accounts for feedforward inputs from retina and intrageniculate interneurons as well as feedback inputs from cortex and the thalamic reticular nucleus and can be used to experimentally test different mechanistic models for the geniculate circuitry. Two examples of this are considered: a purely feedforward model incorporating relay cell inputs from retinal ganglion cells and interneurons, and a model including cortical feedback inhibition of relay cells via intrageniculate interneurons.

1. Introduction

The mathematical models used in neuroscience can be categorized into three types; *descriptive*, *mechanistic*, and *interpretive* (Dayan and Abbott 2001). The purpose of *descriptive* modelling is to summarize experimental data compactly in a mathematical form. In *mechanistic* modelling one attempts to account for nervous system activity on the basis of neuronal morphology, physiology and circuitry. This corresponds to the traditional physics approach to mathematical modelling of natural systems. In *interpretive* modelling the goal is

¹ Author to whom any correspondence should be addressed.

to model the functional roles of neuronal systems, i.e. relating neuronal responses to the task of processing information useful to the animal.

An example of a commonly used descriptive model in visual neuroscience is the difference-of-Gaussians (DOG) model introduced by Rodieck (1965) to describe the spatial aspect of the receptive-field structure in retinal ganglion cells. For such cells the receptive fields are small, roughly circular areas, and they exhibit so called centre-surround antagonism. Rodieck described such receptive fields mathematically as the difference of two circularly symmetric and concentric Gaussians. This choice is mathematically convenient and allowed him to derive an analytical solution for the response to moving bars for such cells. The DOG has also been used to describe receptive fields of relay cells in dorsal lateral geniculate nucleus (dLGN) (Kaplan *et al* 1979, So and Shapley 1981, Dawis *et al* 1984, Norton *et al* 1989, Mukherjee and Kaplan 1995, Uhlrich *et al* 1995). With this approach, however, limited insight is gained on *how* the geniculate circuit modifies spatial receptive-field organization between the retinal and geniculate levels. This question can only be addressed with mechanistic modelling, the topic of this work.

The lack of detailed information about the neuronal circuitry has to a large extent prohibited mechanistic modelling of neuronal circuits in the visual pathway. During the last decades major progress has been made in mapping out the properties of the neurons in the dLGN and their synaptic connections (see, for example, review papers by Sherman and Guillery (1996) and McCormick (1992) and recent books by Steriade *et al* (1997) and Sherman and Guillery (2001)). The dLGN is a, relatively speaking, simple system with few cell types and, compared to cortex, modest divergence and convergence of synaptic connections. This limited complexity makes the construction of mechanistic models less ambiguous and reduces the number of unknown model parameters. Further, since a lot of both *in vivo* and *in vitro* physiological experiments have been done on the dLGN circuit, data are available for falsification of tentative mechanistic models.

Recently, we (Einevoll and Heggelund 2000, Einevoll *et al* 2000) have investigated mechanistic rate-based models to study spatial transfer characteristics of dLGN utilizing data from *in vivo* recordings from cat dLGN with circular-spot stimuli (Ruksenas *et al* 2000). The mechanistic models for the dLGN circuit were based on physiological and anatomical findings, while the descriptive DOG model was used to represent the spatial characteristics of the retinal input. We studied simplified circuit models where a relay cell receives

- (i) direct excitation from a single retinal ganglion cell, and
- (ii) indirect feedforward inhibition from several retinal ganglion cells via intrageniculate interneurons.

Neuronal responses of relay cells and dLGN interneurons to circular spot stimuli were calculated, and the resulting analytical formulae were compared with the recent *in vivo* results of Ruksenas *et al* (2000). Overall, the models were found to account well for the 22 recordings from nonlagged X-cells reported there (both efferent action potentials and afferent S-potentials). Moreover, model predictions for

- (i) receptive-field sizes of interneurons,
- (ii) the amount of centre-surround antagonism for interneurons compared to relay cells, and
- (iii) distance between neighbouring retinal ganglion cells providing input to interneurons,

were all found to be consistent with data available in the literature (Peichl and Wässle 1979, Mastronarde 1992).

Enroth-Cugell and Robson (1966) calculated the spatial frequency response to sinusoidal stimuli for retinal ganglion cells with receptive fields described by the DOG model. This is

the basis of the *spatial frequency analysis* method, which has been widely applied in the study of receptive fields during the last decades (Shapley and Lennie 1985). Frequency response methods were originally developed in electrical engineering as a part of *systems theory*, *filter theory*, and *cybernetics* (Oppenheim and Willsky 1997). In *linear* systems the use of sinusoidal input is particularly useful since each frequency component can be probed independently, and for (approximately) linear systems this input is therefore a popular choice. To analyse the properties of the visual system *in vivo*, stationary or drifting gratings are used as visual stimuli, and typically the first-harmonic component of the neuronal firing rate is measured.

In a thorough study of the *limulus* lateral eye, drifting-grating experiments were used to construct and test a mechanistic model for the limulus retina (Brodie *et al* 1978a, 1978b). In mammals the mathematical interpretation of such experiments has so far been limited to descriptive models (Shapley and Lennie 1985). In this paper we describe how different parts of the retino-geniculo-cortical pathway affect the transformation of neuronal responses from retinal ganglion cells to dLGN relay cells.

Linearity is a central assumption in our mathematical treatment. Since, for example, the feedback to relay cells from cortex and TRN is expected to involve nonlinear as well as linear effects, we do not expect our approach to account for all behaviour of the retino-geniculate circuit. Instead it can be viewed as a linear, and thus readily analysable, entry point into mechanistic models of the geniculate circuit. Given that the X pathway has been found to respond approximately linearly when driven by drifting-grating stimuli (So and Shapley 1981, Cheng *et al* 1995), our formalism should nevertheless be suitable for analysis of the X pathway. The mathematical formalism is based on neuronal firing rates and is applicable to the study of both spatial and temporal properties. In fact, it straightforwardly handles spatio-temporally coupled receptive fields.

A particularly useful feature of using drifting gratings as stimuli is that in a linear, spatially homogeneous theory the *ratio* of the first-harmonic components, the retino-geniculate *transfer ratio*, is independent of the response of the retinal ganglion cell. Therefore, no specific assumptions on the mathematical form of the receptive field of the retinal ganglion cells have to be made when comparing experimental results for this ratio with model results. Fortunately, the retino-geniculate transfer ratio is readily available in experiments since both relay cell action potentials and its retinal input (S-potentials) can be measured in extracellular recordings in dLGN (Kaplan and Shapley 1984).

Both relay cells and interneurons receive afferents from the cortex and thalamic reticular nucleus (TRN) (Sherman and Guillery 2001). These feedback connections were not incorporated in our simplified neuronal circuit used to explain the circular spot data of Ruksenas *et al* (2000); with circular spot stimuli the feedback effects from TRN and cortex are expected to play little role (see discussion in Einevoll and Heggelund (2000)). Feedback is, however, expected to be more important for drifting-grating stimuli (Sillito *et al* 1993, Funke and Eysel 1998, Murphy *et al* 1999) which we consider here. In this work we have therefore included feedback effects both from TRN and cortex in addition to the feedforward circuit considered in Einevoll and Heggelund (2000).

In the next section we will briefly describe the traditional descriptive approach for modelling data from drifting-grating experiments. General expressions of responses of dLGN relay cells and the retino-geniculate transfer ratio are derived in section 3. These expressions are based on the known synaptic coupling scheme between (and within) retina, dLGN, TRN and cortex. In section 4 we give examples of how these transfer ratio expressions can be used to probe specific mechanistic models of geniculate circuitry. Our findings are then discussed in the final section.

2. Descriptive modelling of drifting-grating data

The traditional way of analysing drifting-grating data to study the spatial receptive-field organization of retinal and geniculate cells is by means of the DOG model. For retinal ganglion cells of the X-type Enroth-Cugell and Robson (1966) described the response to a drifting-grating stimulus as

$$R(t) = \iint_{\mathbf{r}} W(\mathbf{r})L(\mathbf{r}, t) d^2r \quad (1)$$

where $W(\mathbf{r})$ is the *point-weighting function* describing the spatial characteristic of the receptive field, and $\mathbf{r} = [x, y]$ is the two-dimensional position vector; the spatial integral over \mathbf{r} extends over all two-dimensional space. The luminance $L(\mathbf{r}, t)$ of a sinusoidal grating pattern drifting in the x -direction is mathematically described by

$$L(\mathbf{r}, t) = L_0[1 + m \cos(2\pi v x - 2\pi f t)], \quad (2)$$

where L_0 is the mean luminance, m is the contrast of the grating, and v and f are the spatial and temporal frequencies of the grating, respectively. The response of the ganglion cell stimulated by a drifting grating is (in the case of an even-symmetry point-weighting function) then found to be (Enroth-Cugell and Robson 1966)

$$R(t) = \text{constant} + L_0 m C(v) \cos(2\pi v x - 2\pi f t), \quad (3)$$

where $C(v)$ is the cosine Fourier transform of the point-weighting function $W(\mathbf{r})$. With the point-weight function given as a DOG (Rodieck 1965), i.e.

$$W(\mathbf{r}) = \frac{A_1}{\pi a_1^2} e^{-r^2/a_1^2} - \frac{A_2}{\pi a_2^2} e^{-r^2/a_2^2}, \quad (4)$$

where $r = |\mathbf{r}|$, $C(v)$ is found to be

$$C(v) = A_1 e^{-\pi^2 a_1^2 v^2} - A_2 e^{-\pi^2 a_2^2 v^2}. \quad (5)$$

Enroth-Cugell and Robson (1966) assumed $C(v)$ to be proportional with contrast sensitivity and fitted the expression in equation (5) with data from contrast-sensitivity tuning curves from experiments with drifting sinusoidal gratings.

This fitting procedure is illustrated in figure 1(a) for a more recent example data set reported by Cheng *et al* (1995, figure 2) for an X relay cell in cat. Here neuronal responses were measured directly, and both relay cell action potentials and so-called S-potentials were recorded. An S-potential is assumed to be a post-synaptic potential that reflects a single-action potential in the retinal afferents (Bishop *et al* 1958, Hubel and Wiesel 1961, Cleland *et al* 1971, Kaplan and Shapley 1984). Following Cheng *et al* (1995), we will assume each S-potential to represent an action potential in a single ganglion cell providing the (dominant) retinal input to the relay cell.

The standard descriptive-modelling procedure for analysing such data has been to separately fit the retinal-input and relay cell spatial frequency tuning curves to the DOG-model expression in equation (5). This provides estimates for both the ganglion and relay cell centre (A_1) and surround (A_2) weights as well as the corresponding width parameters a_1 and a_2 . These fits are shown in figure 1(a), and we observe that the DOG model is able to fit the experimental data well. However, no insight is gained regarding what aspects of the retino-geniculate circuitry are responsible for the differences in neuronal responses between the retinal and geniculate level. For such insight mechanistic, not descriptive, modelling is needed, and this will be the topic of the remainder of this paper.

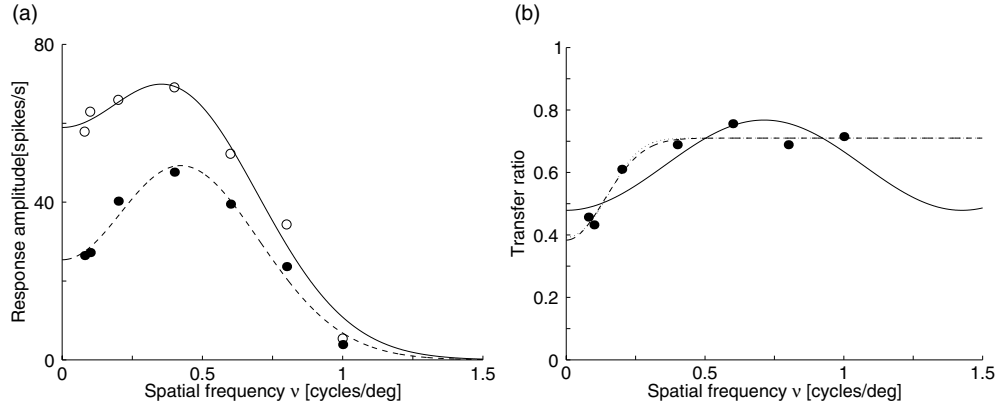


Figure 1. (a) Spatial frequency tuning curves of a dLGN X cell (full dots) and its main retinal drive (S-potentials, open dots). Replotted data from Cheng *et al* (1995, figure 2). Stimulus contrast was 32%, and the temporal frequency was 3.1 Hz. Amplitudes of first-harmonic responses to drifting sinusoidal gratings are shown as functions of spatial frequency. Best fits to the DOG model, equation (5), are shown. (b) Spatial frequency tuning curve for the transfer ratio, i.e. ratio between response amplitudes for relay cells and retinal input, for the data in (a). Solid curve is best fit for the discrete example feedforward model ($B_{ff} = 0.84$, $\eta_{ff} = 0.086$, $r_a = 0.70^\circ$ in equation (33)). Dashed curve is best fit for the feedforward model with Gaussian inhibition ($B_{ff} = 0.71$, $\eta_{ff} = 0.46$, $b_2 = 1.64^\circ$ in equation (34)). Dotted curve is best fit to example feedback model ($B_{fb} = 0.71$, $D_{fb} = 0.81$, $d_{fb} = 1.95^\circ$ in equation (41)).

3. Mechanistic modelling of drifting-grating data for dLGN cells

In this section we will describe a mechanistic modelling approach to interpret data from X-type relay cells from experiments with drifting sinusoidal gratings used as stimuli.

3.1. Input from retinal ganglion cells

Our goal is *not* to do mechanistic modelling of the retinal circuit, and we merely need a descriptive model for the retinal input in the mechanistic model of the dLGN circuit. For this, a slight reformulation of the descriptive modelling described in the previous section is useful.

For a linear retinal ganglion cell at a position \mathbf{r} in the visual field the response, i.e. the firing rate, can be written as

$$\hat{R}_g(\mathbf{r}, t) = \int_{-\infty}^{\infty} \iint_{r_0} G_g(\mathbf{r} - \mathbf{r}_0, \tau) s(\mathbf{r}_0, t - \tau) d^2 r_0 d\tau \quad (6)$$

if one assumes linearity and time invariance. Here, $G_g(\mathbf{r}, \tau)$ is the *spatio-temporal impulse-response function*, directly related to the receptive field of the retinal ganglion cell (Heeger 1991). This integral is essentially a convolution between stimulus and impulse-response functions (Heeger 1991). The assumption of linearity seems to be justified for most X-type ganglion cells, while it is generally not applicable to Y-type cells (Enroth-Cugell and Robson 1966, Hochstein and Shapley 1976). In equation (6), $s(\mathbf{r}, t)$ represents the visual stimulus presented at position $\mathbf{r} = [x, y]$ at time t . The spatial integral over r_0 goes over all two-dimensional space. We have chosen to let the temporal integration go from $\tau = -\infty$ to ∞ to correspond with the general expression for the Fourier transform. From causality it follows that $G_g(\mathbf{r}, \tau < 0) = 0$, so the lower integration boundary in equation (6) could also be set to $\tau = 0$.

With a one-dimensional sinusoidal drifting grating as stimulus, the luminance profile can be described mathematically as (see equation (2))

$$L(\mathbf{r}, t) = L_0[1 + m \cos(\mathbf{k}\mathbf{r} - \omega t + \psi)], \quad (7)$$

where we have introduced the *wavevector* \mathbf{k} and the *angular frequency* ω for mathematical convenience. The wavevector sets the direction and spatial wavelength of the moving grating and is related to the spatial frequency ν via $k = |\mathbf{k}| = 2\pi\nu$. The angular frequency ω is related to the temporal frequency f via $\omega = 2\pi f$. By choosing the time $t = 0$ at an instant where the luminance profile is $L(\mathbf{r}) = L_0(1 + m \cos(\mathbf{k}\mathbf{r}))$, the constant phase factor ψ can be set to zero, and in the following we set $\psi = 0$.

Response versus luminance curves for photoreceptors are typically sigmoidal (Leibovic 1990). This relationship will be reflected in the neuronal activity of the retinal ganglion cells. Following Einevoll and Heggelund (2000) it is convenient to represent the visual stimulus via an (unspecified) sigmoidal activity function of the luminance $L(\mathbf{r})$, i.e. $s(\mathbf{r}) = l(L(\mathbf{r}))$ where l is a sigmoid of some form (Dayan and Abbott 2001). We choose $l(L(\mathbf{r}))$ to have the dimension of firing rate, i.e. spikes/s. With this representation, the sigmoidal nonlinearity is shifted to the input function (stimulus function, $s(\mathbf{r})$), and the assumption of spatial summation of visual inputs via the linear impulse–response function $G_g(\mathbf{r}, t)$ becomes more plausible. Note that the linear choice $s(\mathbf{r}) = L(\mathbf{r})$ would give the traditional expression in equation (1).

With $s(\mathbf{r}_0, t - \tau) = l(L(\mathbf{r}_0, t - \tau))$ inserted into equation (6) the only dependence on luminance lies in the activity function $l(L)$. The shape of this function can be assessed by considering the special case with no luminance modulation, i.e. $m = 0$, which corresponds to diffuse illumination with the mean luminance L_0 . For this situation the linear response corresponds to a response denoted \hat{R}_g^0 , which according to equation (6) is given by

$$\hat{R}_g^0 = l(L_0) \int_{\tau} \iint_{r_0} G_g(\mathbf{r} - \mathbf{r}_0, \tau) d^2r_0 d\tau = l(L_0) \tilde{G}_g(\mathbf{0}, 0). \quad (8)$$

The notation $\tilde{G}_g(\mathbf{0}, 0)$ is used since this constant corresponds to the complex Fourier transform of $G_g(\mathbf{r}, t)$,

$$\tilde{G}_g(\mathbf{k}, \omega) \equiv \int_{\tau} \iint_{\mathbf{u}} e^{-i(\mathbf{k}\mathbf{u} - \omega\tau)} G_g(\mathbf{u}, \tau) d^2u d\tau, \quad (9)$$

for the special case $\mathbf{k} = \mathbf{0}$ and $\omega = 0$. This transform will be used widely in this paper. Within our model $l(L_0) = \hat{R}_g^0 / \tilde{G}_g(\mathbf{0}, 0)$, and consequently the shape of the function $l(L)$ will be identical to the shape of the luminance dependence of the ganglion-cell response to full-field, diffuse illumination ($m = 0$), only scaled by the constant factor $\tilde{G}_g(\mathbf{0}, 0)$. In a linear system this full-field illumination response can also be obtained by temporal averaging of a drifting-grating response ($m \neq 0$) over an integer number of oscillatory periods.

Schematic illustrations of monotonically increasing $l(L)$, applicable to ON-centre cells, and monotonically decreasing $l(L)$, applicable to OFF-centre cells, are shown in figure 2. The function $l(L)$ incorporates the photoreceptor response, which strongly adapts to the level of diffuse illumination (Leibovic 1990), and $l(L)$ will adapt correspondingly. In the present modelling we will, however, assume that the shape of $l(L)$ is constant during the recording of an experimental data set.

The function $l(L)$ is nonlinear, but for small luminance contrasts m , $l(L)$ can be approximated by the two first terms in a Taylor expansion around the mean luminance L_0 , i.e.

$$l(L(\mathbf{r}, t)) \approx l(L_0) + L_0 l'(L_0) m \cos(\mathbf{k}\mathbf{r} - \omega t). \quad (10)$$

This linearization is illustrated in figure 2.

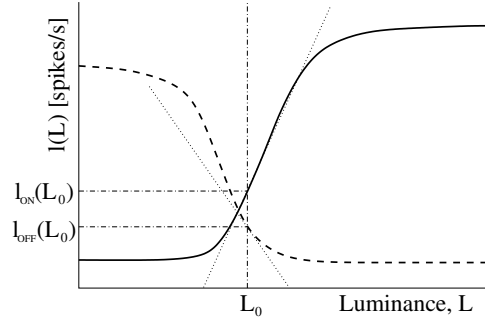


Figure 2. Schematic illustration of possible shapes of activity functions $I(L)$ as functions of luminance L for ON-centre (—) and OFF-centre (- - -) cells. L_0 denotes a mean luminance of a drifting-grating stimulus. Dotted lines illustrate the linear approximation around L_0 given by equation (10).

The ganglion-cell response is then given by

$$\begin{aligned} \hat{R}_g(\mathbf{r}, t) &\approx \int_{\tau} \iint_{r_0} G_g(\mathbf{r} - \mathbf{r}_0, \tau) [l(L_0) + L_0 l'(L_0) m \cos(\mathbf{k}r_0 - \omega(t - \tau))] d^2 r_0 d\tau \\ &= l(L_0) \tilde{G}_g(\mathbf{0}, 0) + L_0 l'(L_0) m \int_{\tau} \iint_{r_0} G_g(\mathbf{r} - \mathbf{r}_0, \tau) \\ &\quad \times \cos(\mathbf{k}r_0 - \omega(t - \tau)) d^2 r_0 d\tau. \end{aligned} \quad (11)$$

We now use the standard mathematical trick of replacing the real function $\cos(\mathbf{k}r_0 - \omega(t - \tau))$ with the complex quantity $\exp(i\mathbf{k}r_0 - i\omega(t - \tau))$ and, correspondingly, the real response function $\hat{R}_g(\mathbf{r}, t)$ with the corresponding complex quantity $R_g(\mathbf{r}, t)$. These are related via $\hat{R}_g(\mathbf{r}, t) = \text{Re}\{R_g(\mathbf{r}, t)\}$ where $\text{Re}\{z\}$ represents the real part of the complex number z . By introducing the auxiliary variable $\mathbf{u} = \mathbf{r} - \mathbf{r}_0$ we find

$$\begin{aligned} R_g(\mathbf{r}, t) &= l(L_0) \tilde{G}_g(\mathbf{0}, 0) + L_0 l'(L_0) m \int_{\tau} \iint_{r_0} G_g(\mathbf{r} - \mathbf{r}_0, \tau) e^{i(\mathbf{k}r_0 - \omega(t - \tau))} d^2 r_0 d\tau \\ &= l(L_0) \tilde{G}_g(\mathbf{0}, 0) + L_0 l'(L_0) m e^{i(\mathbf{k}r - \omega t)} \int_{\tau} \iint_{\mathbf{u}} G_g(\mathbf{u}, \tau) e^{-i(\mathbf{k}\mathbf{u} - \omega\tau)} d^2 \mathbf{u} d\tau \\ &= l(L_0) \tilde{G}_g(\mathbf{0}, 0) + L_0 l'(L_0) m \tilde{G}_g(\mathbf{k}, \omega) e^{i(\mathbf{k}r - \omega t)} \\ &= l(L_0) \tilde{G}_g(\mathbf{0}, 0) + L_0 l'(L_0) m |\tilde{G}_g(\mathbf{k}, \omega)| e^{i(\mathbf{k}r - \omega t + \Phi_g)}, \end{aligned} \quad (12)$$

where we have used the general relationship $\tilde{G}_g(\mathbf{k}, \omega) = |\tilde{G}_g(\mathbf{k}, \omega)| e^{i\Phi_g}$ in the final step. The real-valued ganglion-cell response is thus given by

$$\hat{R}_g(\mathbf{r}, t) = \text{Re}\{R_g(\mathbf{r}, t)\} = l(L_0) \tilde{G}_g(\mathbf{0}, 0) + L_0 l'(L_0) m |\tilde{G}_g(\mathbf{k}, \omega)| \cos(\mathbf{k}r - \omega t + \Phi_g), \quad (13)$$

which is of the same form as equation (3), except for the inclusion of the phase shift Φ_g . However, in our reformulation the term $L_0 C(v)$ in equation (3) is replaced by the product $L_0 l'(L_0) |\tilde{G}_g(\mathbf{k}, \omega)|$, commonly referred to as the *contrast gain* (Watson 1992). The constant mean-activity term is now specified in terms of the activity function $l(L_0)$ and the spatially and temporally summated impulse-response function $\tilde{G}_g(\mathbf{0}, 0)$. Note that ON- and OFF-cells will have $l'(L_0)$ of opposite signs (see figure 2) which means that their sinusoidal responses will be approximately 180° out of phase (provided that their phase shifts Φ_g are not too different).

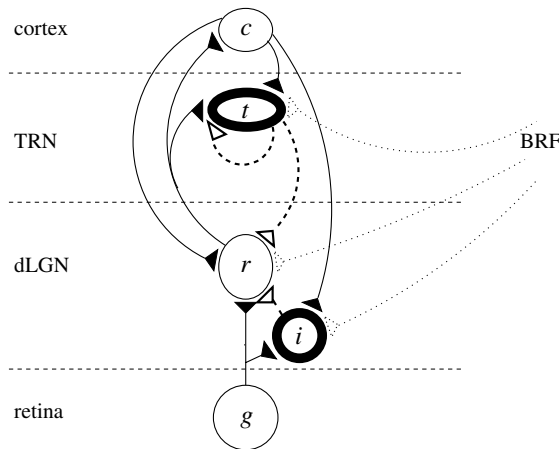


Figure 3. Schematic view of the geniculate circuit for the X pathway. The neurons involved are retinal ganglion cells (g), geniculate relay cells (r), intrageniculate interneurons (i), thalamic reticular cells (t), and cortical cells (c). The excitatory connections are shown as solid curves while the inhibitory connections are shown with dashed curves. In addition the geniculate and thalamic reticular cells receive inputs from the brainstem reticular formation (BRF).

3.2. Relay-cell response functions

The corresponding descriptive-model dLGN relay cell response to drifting gratings is, in analogy with equation (12), given by

$$R_r(\mathbf{r}, t) = l(L_0)\tilde{G}_r(\mathbf{0}, 0) + L_0l'(L_0)m\tilde{G}_r(\mathbf{k}, \omega)e^{i(\mathbf{k}\mathbf{r}-\omega t)}, \quad (14)$$

where $\tilde{G}_r(\mathbf{k}, \omega)$ is the Fourier transform of the spatio-temporal relay cell impulse–response function $G_r(\mathbf{r}, t)$. The form of $G_r(\mathbf{r}, t)$ will depend on the properties of both the retinal and the geniculate circuit.

Our strategy for the mechanistic modelling is to construct the relay cell impulse–response function $\tilde{G}_r(\mathbf{k}, \omega)$ based on current knowledge about the pattern of functional neuronal couplings in dLGN (reviewed by Sherman and Guillery 2001). Relay cells receive excitatory input from retinal ganglion cells as well as feedforward inhibition from intrageniculate interneurons both via dendro-dendritic structures (triads) and (possibly) axonal output. The interneurons in turn receive excitation from a few retinal ganglion cells. In addition, the relay cells receive inhibitory feedback from the TRN and excitatory feedback from the striate cortex. The intrageniculate interneurons and TRN cells also receive excitatory feedback from cortex. All these feedforward and feedback connections will eventually be included in our present mathematical treatment. A schematic view of the circuit is given in figure 3.

3.2.1. Feedforward excitation only. To illustrate the mathematical technique used in this paper more clearly, we first consider a severely simplified model of the geniculate X pathway including only the feedforward excitatory afferents to dLGN relay cells. We assume that the X-type relay cells receive all their feedforward inputs from X-type retinal ganglion cells belonging to the same symmetry class, i.e. only ON-symmetry or only OFF-symmetry inputs (Cleland *et al* 1971, Coenen and Vendrik 1972, Dubin and Cleland 1977, Cleland and Lee 1985, Mastrorarde 1987a, 1987b, 1992). The ON- and OFF-channels are thus decoupled and can be treated separately.

Assuming linearity and time-invariance for the feedforward excitatory couplings between retinal ganglion cells and relay cells, the relay cell response can be written as

$$R_r(\mathbf{r}, t) = \int_{\tau} \iint_{r_0} K_{rg}(\mathbf{r} - \mathbf{r}_0, \tau) R_g(\mathbf{r}_0, t - \tau) d^2 r_0 d\tau, \quad (15)$$

where $K_{rg}(\mathbf{r} - \mathbf{r}_0, \tau)$ is the spatio-temporal retino-geniculate coupling function (coupling kernel) between a retinal ganglion cell at a position \mathbf{r}_0 and a relay cell at \mathbf{r} .

The expression in equation (15) is analogous to the expression in equation (6) with $R_g(\mathbf{r}_0, t - \tau)$ now corresponding to the ‘stimulus’ and $K_{rg}(\mathbf{r} - \mathbf{r}_0, \tau)$ to the impulse–response function. An essential assumption underlying equation (15) is the assumption of *spatial homogeneity*, i.e. that

- (i) all retinal ganglion cells coupled to a relay cell (when more than one) have the same response properties, and
- (ii) the corresponding coupling function K_{rg} depends only on the relative distance between these cells.

Insertion of equation (12) into (15) yields

$$\begin{aligned} R_r(\mathbf{r}, t) &= \int_{\tau} \iint_{r_0} K_{rg}(\mathbf{r} - \mathbf{r}_0, \tau) l(L_0) \tilde{G}_g(\mathbf{0}, 0) d^2 r_0 d\tau \\ &\quad + \int_{\tau} \iint_{r_0} K_{rg}(\mathbf{r} - \mathbf{r}_0, \tau) L_0 l'(L_0) m \tilde{G}_g(\mathbf{k}, \omega) e^{i(\mathbf{k}\mathbf{r}_0 - \omega(t-\tau))} d^2 r_0 d\tau \\ &= l(L_0) \tilde{K}_{rg}(\mathbf{0}, 0) \tilde{G}_g(\mathbf{0}, 0) + L_0 l'(L_0) m \tilde{K}_{rg}(\mathbf{k}, \omega) \tilde{G}_g(\mathbf{k}, \omega) e^{i(\mathbf{k}\mathbf{r} - \omega t)}. \end{aligned} \quad (16)$$

We now have two mathematical expressions for $R_r(\mathbf{r}, t)$, the traditional descriptive one in equation (14) and our new mechanistic one (16). By comparing these expressions we can immediately identify $\tilde{G}_r(\mathbf{0}, 0) = \tilde{K}_{rg}(\mathbf{0}, 0) \tilde{G}_g(\mathbf{0}, 0)$, and the more general relationship

$$\tilde{G}_r(\mathbf{k}, \omega) = \tilde{K}_{rg}(\mathbf{k}, \omega) \tilde{G}_g(\mathbf{k}, \omega). \quad (17)$$

A crucial observation here is that while the drifting-grating response for a relay cell (i.e. the contrast gain) naturally depends on the corresponding response of the retinal ganglion cells feeding into the relay cell, the *ratio* between the harmonically modulated components, $\tilde{T}_{rg}(\mathbf{k}, \omega)$, only depends on the retino-geniculate coupling function \tilde{K}_{rg} , i.e.

$$\tilde{T}_{rg}(\mathbf{k}, \omega) \equiv \frac{L_0 l'(L_0) m \tilde{G}_r(\mathbf{k}, \omega)}{L_0 l'(L_0) m \tilde{G}_g(\mathbf{k}, \omega)} = \frac{\tilde{K}_{rg}(\mathbf{k}, \omega) \tilde{G}_g(\mathbf{k}, \omega)}{\tilde{G}_g(\mathbf{k}, \omega)} = \tilde{K}_{rg}(\mathbf{k}, \omega). \quad (18)$$

Watson (1992) used the term *level transfer function* for a ratio of this type. Here we will call $\tilde{T}_{rg}(\mathbf{k}, \omega)$ the *geniculate transfer function*, and the magnitude $|\tilde{T}_{rg}(\mathbf{k}, \omega)|$ the *geniculate transfer ratio*. The geniculate transfer ratio is given by $|\tilde{T}_{rg}(\mathbf{k}, \omega)| = |\tilde{K}_{rg}(\mathbf{k}, \omega)|$, and the difference in phase between the relay cell and ganglion-cell responses is given by $\Phi_r - \Phi_g = \Phi_{rg} = \arg \tilde{T}_{rg}(\mathbf{k}, \omega) = \arg \tilde{K}_{rg}(\mathbf{k}, \omega)$. Similarly, the ratio of the *mean* responses is found also to be provided by equation (18) for the special case $\mathbf{k} = \mathbf{0}, \omega = 0$, i.e. $\tilde{T}_{rg}^0 = \tilde{K}_{rg}(\mathbf{0}, 0)$.

The observed independence of the geniculate transfer function from the response of the retinal ganglion cell applies to arbitrarily complex model circuits as long as the coupling functions are linear and spatially homogeneous. It should also be noted that the geniculate transfer function is independent of the mean luminance L_0 as well as of the shape of the activity function $l(L_0)$ within our model.

3.2.2. *Feedforward excitation and inhibition.* In addition to feedforward excitatory retinal afferents, the relay cells also receive feedforward inhibition from intrageniculate interneurons which in turn receive excitation from a few retinal ganglion cells (Dubin and Cleland 1977, Mastronarde 1992). As for X-type relay cells we assume that the (X-type) interneurons receive feedforward inputs from X-type retinal ganglion cells of the same symmetry class only. We further assume that the relay cells receive feedforward inhibition from interneurons of the same symmetry class, so that X-ON and X-OFF channels still can be treated independently.

In a linear model the response of an intrageniculate cell to sinusoidal drifting gratings can, in analogy with equation (14), be written as

$$R_i(\mathbf{r}, t) = l(L_0)\tilde{G}_i(\mathbf{0}, 0) + L_0l'(L_0)m\tilde{G}_i(\mathbf{k}, \omega)e^{i(kr-\omega t)}. \quad (19)$$

In analogy with equation (15) we also have

$$\begin{aligned} R_i(\mathbf{r}, t) &= \int_{\tau} \iint_{r_0} K_{ig}(\mathbf{r} - \mathbf{r}_0, \tau) R_g(\mathbf{r}_0, t - \tau) d^2r_0 d\tau \\ &= l(L_0)\tilde{K}_{ig}(\mathbf{0}, 0)\tilde{G}_g(\mathbf{0}, 0) + L_0l'(L_0)m\tilde{K}_{ig}(\mathbf{k}, \omega)\tilde{G}_g(\mathbf{k}, \omega)e^{i(kr-\omega t)}, \end{aligned} \quad (20)$$

and comparing with equation (19) we thus identify $\tilde{G}_i(\mathbf{k}, \omega) = \tilde{K}_{ig}(\mathbf{k}, \omega)\tilde{G}_g(\mathbf{k}, \omega)$. The relay cell response is now given by

$$\begin{aligned} R_r(\mathbf{r}, t) &= \int_{\tau} \iint_{r_0} [K_{rg}(\mathbf{r} - \mathbf{r}_0, \tau) R_g(\mathbf{r}_0, t - \tau) + K_{ri}(\mathbf{r} - \mathbf{r}_0, \tau) R_i(\mathbf{r}_0, t - \tau)] d^2r_0 d\tau \\ &= l(L_0)[\tilde{K}_{rg}(\mathbf{0}, 0)\tilde{G}_g(\mathbf{0}, 0) + \tilde{K}_{ri}(\mathbf{0}, 0)\tilde{K}_{ig}(\mathbf{0}, 0)\tilde{G}_g(\mathbf{0}, 0)] \\ &\quad + L_0l'(L_0)m[\tilde{K}_{rg}(\mathbf{k}, \omega)\tilde{G}_g(\mathbf{k}, \omega) + \tilde{K}_{ri}(\mathbf{k}, \omega)\tilde{K}_{ig}(\mathbf{k}, \omega)\tilde{G}_g(\mathbf{k}, \omega)]e^{i(kr-\omega t)} \\ &= l(L_0)\tilde{G}_r(\mathbf{0}, 0) + L_0l'(L_0)m\tilde{G}_r(\mathbf{k}, \omega)e^{i(kr-\omega t)}, \end{aligned} \quad (21)$$

where we have used equations (14) and (19). The structure of the feedforward retino-geniculate model circuit is as sketched in figure 4, if TRN and all connections to and from it were removed from the diagram.

Comparing the terms in the last two equations in equation (21) we find

$$\tilde{G}_r(\mathbf{k}, \omega) = \tilde{G}_g(\mathbf{k}, \omega)[\tilde{K}_{rg}(\mathbf{k}, \omega) + \tilde{K}_{ri}(\mathbf{k}, \omega)\tilde{K}_{ig}(\mathbf{k}, \omega)]. \quad (22)$$

The geniculate transfer function is thus given by

$$\tilde{T}_{rg}(\mathbf{k}, \omega) = \tilde{K}_{rg}(\mathbf{k}, \omega) + \tilde{K}_{ri}(\mathbf{k}, \omega)\tilde{K}_{ig}(\mathbf{k}, \omega), \quad (23)$$

which still is independent of the response of the retinal ganglion cell.

Equation (23) nicely exposes the beauty of linear systems theory. The geniculate transfer function $\tilde{T}_{rg}(\mathbf{k}, \omega)$, which describes the joint effect of feedforward excitation (first term on the right-hand side of the equation) and indirect feedforward inhibition (second term), is obtained by simply adding the response kernels for the two parallel pathways. The response kernel for the successive effect of excitatory coupling from retina to interneuron, followed by inhibitory coupling of the interneuron to the relay cell, is obtained by multiplying the two pertaining response kernels in Fourier space.

The result in equation (22) could indeed have been written down at once using standard methods of *filter theory*, observing that:

- (i) there are two parallel paths to the relay cells from the ganglion cells, and
- (ii) the parallel path via the interneuron involves a series of two ‘filters’.

More information about filter theory can be found in, for example, the textbooks of Oppenheim and Willsky (1997) and Marmarelis and Marmarelis (1977).

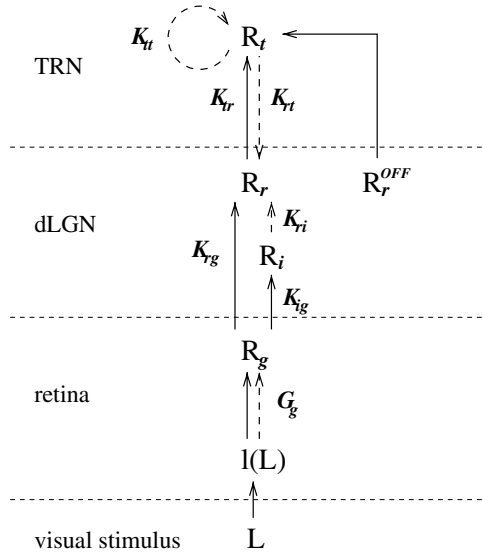


Figure 4. Illustration of mathematical structure of geniculate circuit model including feedforward connections and feedback from TRN. R_g , R_r , R_i , and R_t represent the responses of retinal ganglion cells, relay cells, intrageniculate interneurons, and reticular cells. K_{rg} , K_{ig} , K_{ri} , K_{tr} , K_{rt} , and K_{tt} represent coupling functions as described in the text. The excitatory connections are shown as solid lines while the inhibitory connections are shown with dashed lines.

3.2.3. *Feedback from thalamic reticular nucleus.* On the way to cortex the relay cell axons send out lateral arborizations which provide retinotopic excitation of the TRN. These inhibitory cells have retinotopic connections with relay cells as well as lateral inhibitory connections with other reticular (TRN) cells. The separation of the X and Y pathway appears to hold also for reticular cells (Lindström and Wróbel 1990), whence we neglect any influence from the Y pathway in the present X-pathway model. However, the reticular cells exhibit mixed ON–OFF response (Ahlsén *et al* 1983, Dubin and Cleland 1977, Funke and Eysel 1998) and presumably receive inputs from both relay ON-cells and relay OFF-cells (Ahlsén *et al* 1983).

Below we describe the outcome of the derivation of an expression for the geniculate transfer ratio for X-ON cells, an expression which is straightforwardly modified to obtain the corresponding ratio for X-OFF cells. A complete mathematical derivation is given in appendix A.

Since the TRN cells receive mixed ON and OFF inputs, their response is affected by both the functions $l_{ON}(L_0)$ and $l_{OFF}(L_0)$, see figure 2. With our focus on the ON-ratio, it is mathematically convenient to write the descriptive expression for a TRN cell to drifting gratings, in analogy with equation (14), as

$$R_t(\mathbf{r}, t) = l_{ON}(L_0)\tilde{G}_t(\mathbf{0}, 0) + L_0 l'_{ON}(L_0)m\tilde{G}_t(\mathbf{k}, \omega)e^{i(\mathbf{k}\mathbf{r} - \omega t)}. \quad (24)$$

In analogy with equation (15) we now have

$$R_t(\mathbf{r}, t) = \int_{\tau} \iint_{r_0} [K_{tr}^{ON}(\mathbf{r} - \mathbf{r}_0, \tau)R_r^{ON}(\mathbf{r}_0, t - \tau) + K_{tr}^{OFF}(\mathbf{r} - \mathbf{r}_0, \tau)R_r^{OFF}(\mathbf{r}_0, t - \tau) + K_{tt}(\mathbf{r} - \mathbf{r}_0, \tau)R_t(\mathbf{r}_0, t - \tau)] d^2r_0 d\tau. \quad (25)$$

Here $K_{tr}^{ON}(\mathbf{r} - \mathbf{r}_0, \tau)$ ($K_{tr}^{OFF}(\mathbf{r} - \mathbf{r}_0, \tau)$) is the spatio-temporal coupling function describing the excitatory influence of a relay ON-cell (OFF-cell) on a TRN cell, and $K_{tt}(\mathbf{r} - \mathbf{r}_0, \tau)$ is correspondingly describing the coupling function between two TRN cells, cf figure 4.

We now make the assumption that the ON- and OFF-channels are identical except for the difference in the functions $l_{\text{OFF}}(L_0)$ and $l_{\text{ON}}(L_0)$. Mathematically this corresponds to $\tilde{K}_{\text{tr}}^{\text{ON}}(\mathbf{k}, \omega) = \tilde{K}_{\text{tr}}^{\text{OFF}}(\mathbf{k}, \omega) \equiv \tilde{K}_{\text{tr}}(\mathbf{k}, \omega)$ and $\tilde{G}_{\text{r}}^{\text{ON}}(\mathbf{k}, \omega) = \tilde{G}_{\text{r}}^{\text{OFF}}(\mathbf{k}, \omega) \equiv \tilde{G}_{\text{r}}(\mathbf{k}, \omega)$. This assumption also implies that G_{g} , K_{rg} , K_{ri} , and K_{ig} are the same for the two channels.

Mathematical analysis then yields the following for the Fourier-transformed impulse-response functions of the TRN cells:

$$\begin{aligned}\tilde{G}_{\text{t}}(\mathbf{0}, 0) &= \frac{\tilde{K}_{\text{tr}}(\mathbf{0}, 0)\tilde{G}_{\text{r}}(\mathbf{0}, 0)[1 + c_0(L_0)]}{1 - \tilde{K}_{\text{tt}}(\mathbf{0}, 0)}, \\ \tilde{G}_{\text{t}}(\mathbf{k}, \omega) &= \frac{\tilde{K}_{\text{tr}}(\mathbf{k}, \omega)\tilde{G}_{\text{r}}(\mathbf{k}, \omega)[1 - c_1(L_0)]}{1 - \tilde{K}_{\text{tt}}(\mathbf{k}, \omega)}, \quad [\mathbf{k}, \omega] \neq [\mathbf{0}, 0],\end{aligned}\quad (26)$$

where we have introduced the functions

$$c_0(L_0) \equiv l_{\text{OFF}}(L_0)/l_{\text{ON}}(L_0), \quad c_1(L_0) \equiv -l'_{\text{OFF}}(L_0)/l'_{\text{ON}}(L_0). \quad (27)$$

Here we see that due to the mixing of the ON- and OFF-channels, the quantities $\tilde{G}_{\text{t}}(\mathbf{0}, 0)$ and $\tilde{G}_{\text{t}}(\mathbf{k}, \omega)$ depend on the luminance L_0 via the functions $c_0(L_0)$ and $c_1(L_0)$, respectively. We note in passing that since the ON- and OFF-channels are approximately 180° out of phase, the sinusoidally modulated inputs to reticular cells from the relay ON- and OFF-cells will tend to cancel each other. This follows from the fact that $l'(L_0)$ of the ON- and OFF-channels have opposite signs, as seen in figure 2. In fact, if $l'_{\text{OFF}}(L_0) = -l'_{\text{ON}}(L_0)$, so that $c_1(L_0) = 1$, the reticular cells will receive no modulated input at all; the modulation of their response should then vanish as well, even if the cells operate quite nonlinearly in general.

Note that the division by $1 - \tilde{K}_{\text{tt}}(\mathbf{k}, \omega)$ in equation (26) is another standard result of linear filter theory: feedback loops have a divisive effect and can give rise to singularities in the response and transfer functions, i.e. can show resonances.

The retino-geniculate transfer function in the presence of reticular feedback can now be derived by similar reasoning as applied in the previous sections. We therefore refer the reader to appendix A for details and give here merely the results. The retino-geniculate transfer function for the *modulated* response is given by

$$\tilde{T}_{\text{rg}}(\mathbf{k}, \omega; L_0) = \frac{\tilde{K}_{\text{rg}}(\mathbf{k}, \omega) + \tilde{K}_{\text{ri}}(\mathbf{k}, \omega)\tilde{K}_{\text{ig}}(\mathbf{k}, \omega)}{1 - \frac{\tilde{K}_{\text{ri}}(\mathbf{k}, \omega)\tilde{K}_{\text{tr}}(\mathbf{k}, \omega)[1 - c_1(L_0)]}{1 - \tilde{K}_{\text{tt}}(\mathbf{k}, \omega)}}. \quad (28)$$

Note that in contrast to the geniculate transfer function for the feedforward model in equation (23), this transfer functions depends on the mean luminance L_0 via the function $c_1(L_0)$. This reflects that the modulatory drives, $l'(L_0)$, to the ON- and OFF-channels in the circuit will vary with the luminance as illustrated in figure 2.

Correspondingly, the transfer ratio for the *mean* response is given by

$$\tilde{T}_{\text{rg}}(\mathbf{0}, 0; L_0) = \frac{\tilde{K}_{\text{rg}}(\mathbf{0}, 0) + \tilde{K}_{\text{ri}}(\mathbf{0}, 0)\tilde{K}_{\text{ig}}(\mathbf{0}, 0)}{1 - \frac{\tilde{K}_{\text{ri}}(\mathbf{0}, 0)\tilde{K}_{\text{tr}}(\mathbf{0}, 0)[1 + c_0(L_0)]}{1 - \tilde{K}_{\text{tt}}(\mathbf{0}, 0)}}, \quad (29)$$

which also depends on the mean luminance via the function $c_0(L_0)$. Note that all quantities in this equation are real.

The transfer function for the modulated response in equation (28) no longer becomes identical to the mean-response transfer ratio in equation (29) in the limit $\mathbf{k} \rightarrow \mathbf{0}$, $\omega \rightarrow 0$, due to the mixing of ON- and OFF-channels via feedback from reticular cells.

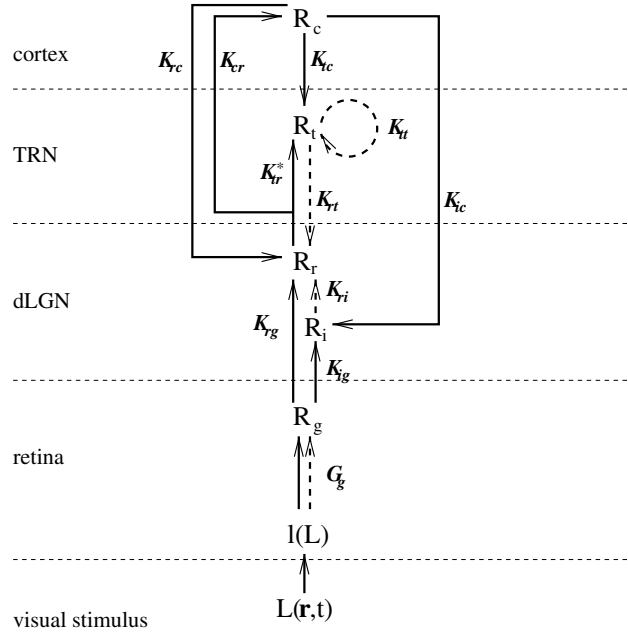


Figure 5. Schematic illustration of the model geniculate circuit. R_g , R_r , R_i , R_t , and R_c represent the responses of retinal ganglion cells, relay cells, interneurons, reticular cells, and cortical cells, respectively. K_{mn} ($m, n = g, i, r, t, c$) represents the coupling from neurons of type n on neurons of type m as described in the text. K_{tr}^* represents the accumulated effect of input to reticular cells from both relay ON and relay OFF cells (see figure 4 and text). Excitatory connections are shown as solid lines while the inhibitory connections are shown with dashed lines.

3.2.4. Extended geniculate circuit. Relay cells, intrageniculate interneurons and TRN cells receive excitatory afferents from layer VI of the striate cortex. These cortical projections are, in the anatomical sense at least, the major input to the dLGN and are broadly retinotopically organized (Sillito and Jones 1997). The present modelling approach can also be extended to include the effect from cortical feedback. However, the output from these layer VI cells is a result of complex cortical processing of the geniculate inputs, and the effect of cortical feedback must be incorporated in a descriptive manner. An additional complication is that the cortical cells in layer VI have orientation-tuned receptive fields. A natural approach could thus be to include a set of different cortical neuronal populations in our model, each representing neurons tuned to a particular orientation. Then, depending on the orientation of the drifting grating, a subset of these neuronal populations would be activated. Instead we will lump all these populations into a single cortical neuronal population *without* orientation specificity.

For the extended geniculate circuit including all feedforward and feedback afferents shown in figure 5, we show in Appendix B that the geniculate transfer function in our linear model is given by

$$\tilde{T}_{\text{rg}}(\mathbf{k}, \omega; L_0) = \frac{\tilde{K}_{\text{rg}}(\mathbf{k}, \omega) + \tilde{K}_{\text{ri}}(\mathbf{k}, \omega)\tilde{K}_{\text{ig}}(\mathbf{k}, \omega)}{1 - \tilde{K}_{\text{rc}}(\mathbf{k}, \omega)\tilde{K}_{\text{cr}}(\mathbf{k}, \omega) - \tilde{K}_{\text{ri}}(\mathbf{k}, \omega)\tilde{K}_{\text{ic}}(\mathbf{k}, \omega)\tilde{K}_{\text{cr}}(\mathbf{k}, \omega) - \frac{\tilde{K}_{\text{ri}}(\mathbf{k}, \omega)\tilde{K}_{\text{tr}}^*(\mathbf{k}, \omega; L_0) + \tilde{K}_{\text{ri}}(\mathbf{k}, \omega)\tilde{K}_{\text{ic}}(\mathbf{k}, \omega)\tilde{K}_{\text{cr}}(\mathbf{k}, \omega)}{1 - \tilde{K}_{\text{ri}}(\mathbf{k}, \omega)}}} \quad (30)$$

where the symbols are explained in figure 5. Here we have introduced the shorthand notation $\tilde{K}_{\text{tr}}^*(\mathbf{k}, \omega; L_0) \equiv \tilde{K}_{\text{tr}}(\mathbf{k}, \omega)[1 - c_1(L_0)]$. The transfer function depends on the mean luminance

L_0 due to the mixed ON–OFF input to reticular cells. Such mixing is also expected to be induced by the cortical feedback, even if this luminance dependence is not stated explicitly in the expression. Only if feedback is neglected is the transfer function expected to be independent of both the mean luminance and the shape of the activity function $l(L_0)$.

The transfer ratio for the mean response $\tilde{T}_{\text{rg}}(\mathbf{0}, 0; L_0)$ has identical form with the geniculate transfer function in equation (30) with $[\mathbf{0}, 0]$ replacing $[\mathbf{k}, \omega]$ and $\tilde{K}_{\text{tr}}^*(\mathbf{0}, 0; L_0) \equiv \tilde{K}_{\text{tr}}(\mathbf{0}, 0)[1 + c_0(L_0)]$.

Even if the final expression for the geniculate transfer function in equation (30) is quite extended, it has a simple structure. The direct feedforward excitation and the indirect feedforward inhibition via interneurons are represented by the first and second terms in the numerator, respectively. The feedback effects are accounted for in the denominator. Here the second term accounts for the direct excitatory feedback loop between relay cells and cortex, the third term for inhibition via the relay–cortex–interneuron–relay loop, and the fourth term for feedback effects mediated by TRN cells.

4. Example applications

The previous section provides the necessary theoretical framework for probing the retino-geniculate circuitry by applying data from traditional experiments with drifting sinusoidal gratings. When combined with mechanistic model expressions for the coupling functions $K(\mathbf{r}, t)$, the general transfer-function expression in equation (30) (or reduced versions of it) gives mechanistic expressions for the geniculate transfer ratio. These theoretical transfer ratios can then be compared with experimental data.

4.1. Spatial transfer

To illustrate how the method can be used to probe the spatial properties we will consider data reported by Cheng *et al* (1995, figure 2) for an X relay cell in cat. The experimental data for the first-harmonic responses of relay cells (action potentials) and their retinal input (S-potentials) are shown in figure 1(a). The standard descriptive way to analyse such data has been outlined in section 2. The alternative method suggested by the present theoretical work is to

- (i) replot the experimental data to provide spatial frequency curves for the geniculate transfer ratio, and
- (ii) fit this curve to the relevant theoretical expressions.

The spatial frequency tuning curve for the geniculate transfer ratio, i.e. ratio between amplitudes of the modulated relay cell and retinal input responses, for the response data in figure 1(a) is shown in figure 1(b).

4.1.1. Feedforward excitation and inhibition. As a first example we consider the feedforward circuit where the feedback from the TRN and cortical cells are neglected, i.e. $K_{\text{rt}} = K_{\text{rc}} = K_{\text{it}} = K_{\text{ic}} = 0$. Relay cells receive excitatory input from a single or a few retinal ganglion cells (Cleland *et al* 1971, Coenen and Vendrik 1972, Cleland and Lee 1985, Mastronarde 1987a, 1987b, 1992). They also receive feedforward inhibition from intrageniculate interneurons which in turn receive excitation from a few retinal ganglion cells (Dubin and Cleland 1977, Mastronarde 1992). Following Einevoll and Heggelund (2000) we thus consider a simplified feedforward circuit model where a relay cell receives

- (i) direct excitation from a single retinal ganglion cell, and
- (ii) indirect feedforward inhibition from several retinal ganglion cells via intrageniculate interneurons.

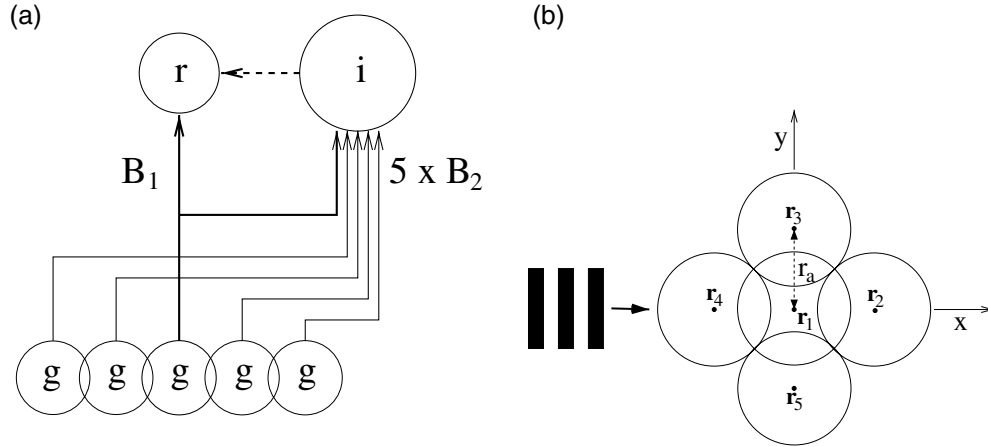


Figure 6. (a) Schematic illustration of couplings at the geniculate level assumed in the discrete model with a single excitatory input with weight B_1 and five inputs to a single interneuron (i). The five (indirect) inhibitory couplings between retinal ganglion (g) and relay cells (r) are each assumed to have weight B_2 . (b) Illustration of model for spatial distribution of inputs from retinal ganglion cells to interneuron. The circles represent the receptive-field centres of the five ganglion cells providing input to the interneuron.

The relevant geniculate transfer function is thus of the form given by equation (23).

For mathematical simplicity we assume that all the coupling functions are spatio-temporally separable, i.e. $K_{rg}(\mathbf{r}, t) = f_{rg}(\mathbf{r})h_{rg}(t)$, $K_{ig}(\mathbf{r}, t) = f_{ig}(\mathbf{r})h_{ig}(t)$, and $K_{ri}(\mathbf{r}, t) = f_{ri}(\mathbf{r})h_{ri}(t)$, so that $\tilde{K}(\mathbf{k}, \omega) = \tilde{f}(\mathbf{k})\tilde{h}(\omega)$. For the same reason we further assume that $\tilde{h}_{ri}(\omega)\tilde{h}_{ig}(\omega) \approx \tilde{h}_{rg}(\omega)$ for the relevant temporal frequencies. Throughout this paper we will choose the temporal coupling functions to be normalized, i.e. $\int_{-\infty}^{\infty} h(\tau) d\tau = \int_0^{\infty} h(\tau) d\tau = 1$, so that the synaptic weight is incorporated in the spatial coupling function $f(\mathbf{r})$.

With these assumptions the geniculate transfer function is found to be

$$\tilde{T}_{rg}(\mathbf{k}, \omega) = \tilde{K}_{rg}(\mathbf{k}, \omega) + \tilde{K}_{ri}(\mathbf{k}, \omega)\tilde{K}_{ig}(\mathbf{k}, \omega) \approx [\tilde{f}_{rg}(\mathbf{k}) + \tilde{f}_{ri}(\mathbf{k})\tilde{f}_{ig}(\mathbf{k})]\tilde{h}_{rg}(\omega). \quad (31)$$

The separation of $\tilde{T}_{rg}(\mathbf{k}, \omega)$ into a product of two functions depending on \mathbf{k} and ω , respectively, shows that this geniculate transfer function is spatio-temporally separable.

To find the spatial part of the transfer function we must also make specific choices for the spatial distributions of inputs involved in the indirect feedforward inhibition of relay cells ($f_{ig}(\mathbf{r})$, $f_{ri}(\mathbf{r})$). Several choices of spatial distributions of feedforward inhibition were considered by Einevoll and Heggelund (2000) in the modelling of responses to flashing circular spots. However, the main focus was on a *discrete* model with a finite number of retinal ganglion-cell inputs to the dLGN interneurons. This model assumed that

- (i) the retinal ganglion cell which provides the excitatory input (with weight B_1) to the relay cell is also functionally coupled to an interneuron providing inhibition on the same relay cell,
- (ii) four ‘neighbouring’ ganglion cells, all with receptive fields centred at the same distance r_a from the relay cell receptive-field centre, also give direct excitatory input to this interneuron, and
- (iii) the five excitatory inputs to the interneuron have the same strength.

This discrete model is illustrated in figure 6.

For this model the geniculate transfer function for gratings moving along any of the major axes (x or y , see figure 6(b)) is found to be

$$\begin{aligned}\tilde{T}_{\text{rg}}(\mathbf{k}, \omega) &= [\tilde{f}_{\text{rg}}(\mathbf{k}) + \tilde{f}_{\text{ri}}(\mathbf{k})\tilde{f}_{\text{ig}}(\mathbf{k})]\tilde{h}_{\text{rg}}(\omega) \\ &= \tilde{h}_{\text{rg}}(\omega) \iint_{\mathbf{r}} e^{-i\mathbf{k}\mathbf{r}} \left[B_1\delta(\mathbf{r}) - B_2 \sum_{j=1}^5 \delta(\mathbf{r}-\mathbf{r}_j) \right] d^2r \\ &= \tilde{h}_{\text{rg}}(\omega)[B_1 - B_2(3 + 2\cos(kr_a))],\end{aligned}\quad (32)$$

where $k = |\mathbf{k}|$, and the sum goes over all the five retinal inputs to the interneuron illustrated in figure 6. $\delta(\mathbf{r})$ is the Dirac delta function, and we have used that the Fourier transform of this function is 1.

The experimentally accessible geniculate transfer ratio is given by the amplitude of $\tilde{T}_{\text{rg}}(\mathbf{k}, \omega)$. The data of Cheng *et al* (1995) plotted in figure 1 are taken for a fixed temporal frequency, i.e. a fixed $f = f_0$ (where $f = \omega/2\pi$). Thus the amplitude of the temporal part of the geniculate transfer function gives a fixed positive constant $B_t \equiv |\tilde{h}_{\text{rg}}(2\pi f_0)|$. The wavevector \mathbf{k} is related to the spatial frequency ν used in figure 1 via $k = |\mathbf{k}| = 2\pi\nu$. The theoretical expression for the geniculate transfer ratio to compare with the data in figure 1(b) is thus

$$|\tilde{T}_{\text{rg}}(\nu, f_0)| = B_{\text{ff}}[1 - \eta_{\text{ff}}(3 + 2\cos(2\pi\nu r_a))] \quad (33)$$

where we have introduced the new parameters $B_{\text{ff}} \equiv B_t B_1$ and $\eta_{\text{ff}} \equiv B_2/B_1$. We have also assumed $\eta_{\text{ff}} < 1$, i.e. the overall geniculate inhibition is weaker than the excitation. We see that this model, with its (unrealistic) perfectly symmetric spatial distribution of interneuron inputs, predicts an oscillatory geniculate transfer ratio as function of spatial frequency.

The resulting fit with the present example data from Cheng *et al* (1995, figure 2) is shown in figure 1(b) (solid curve). Fitted parameter values are given in the figure caption. As seen in figure 1(b) the best fit of this discrete feedforward model shows poor agreement with the present example data.

In Kocbach *et al* (2001) other models for feedforward inhibition have been explored, among them a continuous feedforward Gaussian model for the inhibition. Mathematically this corresponds to a total feedforward spatial coupling given by $f(\mathbf{r}) = B_1\delta(\mathbf{r}) - B_2 \exp(-r^2/b_2^2)/(\pi b_2^2)$. Then in analogy to equation (33) one finds for the geniculate transfer ratio for *all* directions of \mathbf{k} :

$$|\tilde{T}_{\text{rg}}(\nu, f_0)| = |\tilde{h}_{\text{rg}}(2\pi f_0)| |B_1 - B_2 e^{-\pi^2 \nu^2 b_2^2}| = B_{\text{ff}}[1 - \eta_{\text{ff}} e^{-\pi^2 \nu^2 b_2^2}]. \quad (34)$$

As shown in figure 1(b) (dashed curve) this model gives a reasonably good fit to the example data from Cheng *et al* (1995, figure 2).

4.1.2. Feedback inhibition. There are several possible channels for feedback inhibition of relay cells in the retino-geniculate circuit shown in figure 3. One possibility is the feedback loop in which relay cells excite reticular (TRN) cells, which in turn inhibit the relay cells (Lo and Sherman 1994). Another possibility is the cortical feedback excitation of interneurons (alternatively, reticular cells) which in turn results in increased inhibitory action on the relay cells. This latter effect has been clearly observed in drifting-grating experiments, as reviewed by Sillito and Jones (1997). We will here consider the inhibitory cortical-feedback channel via interneurons and neglect the reticular cells in the following example. To make the mathematical derivations more transparent we will also for simplicity neglect

- (i) the cortical feedback excitation of relay cells, i.e. $K_{\text{rc}} = 0$, and
- (ii) the feedforward inhibition modelled in the previous section, i.e. $K_{\text{ig}} = 0$.

This model thus focuses on the effects on the shape of the difference in spatial tuning curves between the retinal and geniculate levels on the basis of cortical feedback inhibition on relay cells mediated by interneurons.

For this example model, the general expression for the geniculate transfer function in equation (30) reduces to

$$\tilde{T}_{\text{rg}}(\mathbf{k}, \omega) = \frac{\tilde{K}_{\text{rg}}(\mathbf{k}, \omega)}{1 - \tilde{K}_{\text{ri}}(\mathbf{k}, \omega)\tilde{K}_{\text{ic}}(\mathbf{k}, \omega)\tilde{K}_{\text{cr}}(\mathbf{k}, \omega)}. \quad (35)$$

For the sake of mathematical simplicity we further assume that the coupling functions K_{cr} , K_{ic} , and K_{ri} are spatio-temporally separable, i.e. $K_{\text{cr}}(\mathbf{r}, t) = f_{\text{cr}}(\mathbf{r})h_{\text{cr}}(t)$, $K_{\text{ic}}(\mathbf{r}, t) = f_{\text{ic}}(\mathbf{r})h_{\text{ic}}(t)$, and $K_{\text{ri}}(\mathbf{r}, t) = f_{\text{ri}}(\mathbf{r})h_{\text{ri}}(t)$.

We then find

$$\tilde{T}_{\text{rg}}(\mathbf{k}, \omega) \approx \frac{B_1 \tilde{h}_{\text{rg}}(\omega)}{1 - \tilde{f}_{\text{ri}}(\mathbf{k})\tilde{f}_{\text{ic}}(\mathbf{k})\tilde{f}_{\text{cr}}(\mathbf{k})\tilde{h}_{\text{ri}}(\omega)\tilde{h}_{\text{ic}}(\omega)\tilde{h}_{\text{cr}}(\omega)}, \quad (36)$$

where B_1 still is the weight of the single excitatory retinal afferent.

Since $\tilde{T}_{\text{rg}}(\mathbf{k}, \omega)$ in this expression obviously cannot be written as a product of a function of \mathbf{k} with a function of ω , one immediately sees that even with spatio-temporally separable coupling functions, the geniculate transfer function will be spatio-temporally coupled. Consequently, the relay cell response will also be spatio-temporally coupled since $\tilde{R}_{\text{r}}(\mathbf{k}, \omega) = \tilde{T}_{\text{rg}}(\mathbf{k}, \omega)\tilde{R}_{\text{g}}(\mathbf{k}, \omega)$. This conclusion will hold for all geniculate models incorporating feedback.

A mathematically convenient assumption is to model the spatial coupling functions as Gaussians, i.e.

$$f_{\text{cr}}(\mathbf{r}) = \frac{D_{\text{cr}}}{\pi d_{\text{cr}}^2} e^{-r^2/d_{\text{cr}}^2}, \quad f_{\text{ic}}(\mathbf{r}) = \frac{D_{\text{ic}}}{\pi d_{\text{ic}}^2} e^{-r^2/d_{\text{ic}}^2}, \quad f_{\text{ri}}(\mathbf{r}) = -\frac{D_{\text{ri}}}{\pi d_{\text{ri}}^2} e^{-r^2/d_{\text{ri}}^2}, \quad (37)$$

so that

$$\tilde{f}_{\text{cr}}(\mathbf{k}) = D_{\text{cr}} e^{-k^2 d_{\text{cr}}^2/4}, \quad \tilde{f}_{\text{ic}}(\mathbf{k}) = D_{\text{ic}} e^{-k^2 d_{\text{ic}}^2/4}, \quad \tilde{f}_{\text{ri}}(\mathbf{k}) = -D_{\text{ri}} e^{-k^2 d_{\text{ri}}^2/4}. \quad (38)$$

Here the weight parameters D_{cr} , D_{ic} and D_{ri} are assumed positive, and the negative sign in f_{ri} , the spatial coupling function from interneurons to relay cells, follows from the inhibitory effect on the relay cells from these cells. The geniculate transfer function is then given by

$$\tilde{T}_{\text{rg}}(\mathbf{k}, \omega) = \frac{B_1 \tilde{h}_{\text{rg}}(\omega)}{1 + D_{\text{ri}} D_{\text{ic}} D_{\text{cr}} e^{-k^2 (d_{\text{ri}}^2 + d_{\text{ic}}^2 + d_{\text{cr}}^2)/4} \tilde{h}_{\text{ri}}(\omega)\tilde{h}_{\text{ic}}(\omega)\tilde{h}_{\text{cr}}(\omega)}. \quad (39)$$

The temporal part of the coupling function between ganglion and relay cells in the numerator of equation (39) will only give the multiplicative factor $|\tilde{h}_{\text{rg}}(\omega)|$ in the model expression for the geniculate transfer ratio. However, since $h(\omega)$ in general is a complex number, the temporal functions in the denominator will not generally factor out in a simple way as in the feedforward case.

In the experiments of Cheng *et al* (1995) the temporal frequency was kept fixed at $f_0 = 3.1$ Hz which corresponds to an angular frequency of $\omega_0 = 2\pi f_0 = 20$ s⁻¹. The axonal delays, membrane constants and durations of EPSPs and IPSPs in the circuit are typically less than 10 ms (although the presence of metabotropic receptors indicates that there are exceptions, see Sherman and Guillery (2001)). For temporal coupling functions which are non-negligible only for small time windows around 0 we find

$$\tilde{h}(\omega_0) = \int_{-\infty}^{\infty} e^{i\omega_0 \tau} h(\tau) d\tau \approx \int_{-\infty}^{\infty} h(\tau) d\tau = 1. \quad (40)$$

Here we have assumed that $\exp(i\omega_0\tau) \approx 1 + i\omega_0\tau \approx 1$ and used that $h(t)$ is normalized. For a typical temporal width of $h(t)$ of 5 ms, the approximation error is of the order of $\omega_0\tau \approx 0.1$.

With these simplifications the geniculate transfer ratio for our feedback model, which should be compared with the example data in figure 1(b), is given by

$$|\tilde{T}_{\text{rg}}(v, f_0)| = \left| \frac{B_1 \tilde{h}_{\text{rg}}(2\pi f_0)}{1 + D_{\text{ri}} D_{\text{ic}} D_{\text{cr}} e^{-\pi^2 v^2 (d_{\text{ri}}^2 + d_{\text{ic}}^2 + d_{\text{cr}}^2)}} \right| = \frac{B_{\text{fb}}}{1 + D_{\text{fb}} e^{-\pi^2 v^2 d_{\text{fb}}^2}}, \quad (41)$$

where we have introduced the new parameters $B_{\text{fb}} \equiv B_1 |\tilde{h}_{\text{rg}}(2\pi f_0)|$, $D_{\text{fb}} \equiv D_{\text{ri}} D_{\text{ic}} D_{\text{cr}}$, and $d_{\text{fb}} \equiv (d_{\text{ri}}^2 + d_{\text{ic}}^2 + d_{\text{cr}}^2)^{1/2}$. The three parameters B_{fb} , D_{fb} , and d_{fb} can for our example data be determined by fitting this theoretical function to the data points in figure 1(b) as in the previous feedforward cases. The resulting best fit is shown in this figure as a dotted line with the optimal parameters listed in the figure caption. As seen here the best fit for the feedback model is equally good as the continuous feedforward model, and significantly better than for our discrete feedforward model. The number of fitting parameters is three in all cases.

4.2. Spatio-temporal transfer

Our approach is not limited to testing against drifting-grating data where only the spatial frequency of the grating is varied while the temporal frequency is fixed. Alternatively, we can consider the opposite case where the spatial frequency is fixed while the temporal frequency is varied. Ideally, though, the transfer ratio should be measured as a function of both spatial and temporal frequencies.

To test our modelling approach against such data we need model expressions for the temporal coupling kernels $h(t)$. The simplest choice is a delayed Dirac delta function, $h(t) = \delta(t - \Delta)$, which corresponds to a combined axonal and synaptic delay of Δ without any temporal dispersion.

A more realistic model is the delayed exponential coupling kernel (delayed RC filter) which, properly normalized to 1, is given by

$$h_{\text{RC}}(t) = \Theta(t - \Delta) \frac{1}{\tau} e^{-(t-\Delta)/\tau}, \quad (42)$$

where $\Theta(t)$ is the Heaviside unit step function. The Fourier transform of this kernel is

$$\tilde{h}_{\text{RC}}(\omega) = \int_{-\infty}^{\infty} h_{\text{RC}}(\tau) e^{i\omega\tau} d\tau = \frac{e^{i\Delta\omega}}{1 - i\tau\omega}. \quad (43)$$

To illustrate how feedforward and feedback connections may reveal themselves in the transfer ratio, we show in figure 7 contour plots of the transfer ratio as function of both the spatial and temporal grating frequencies for the delayed exponential model. For the *feedforward* case we use the Gaussian-inhibition model as spatial kernel, whence the transfer function is obtained by combining equations (34) and (43):

$$\tilde{T}_{\text{rg}}(v, f) = \frac{B_{\text{ff}} e^{i2\pi\Delta f}}{1 - i2\pi\tau f} (1 - \eta_{\text{ff}} e^{-\pi^2 v^2 b_2^2}), \quad (44)$$

where we use the temporal frequency f instead of the angular frequency ω .

The corresponding expression for a system with feedback is obtained by

- (i) assuming $\tilde{h}_{\text{ri}}(\omega)\tilde{h}_{\text{ic}}(\omega)\tilde{h}_{\text{cr}}(\omega) = \tilde{h}_{\text{RC}}(\omega)$ and
- (ii) neglecting the feedforward temporal coupling term $\tilde{h}_{\text{rg}}(\omega)$ in equation (36).

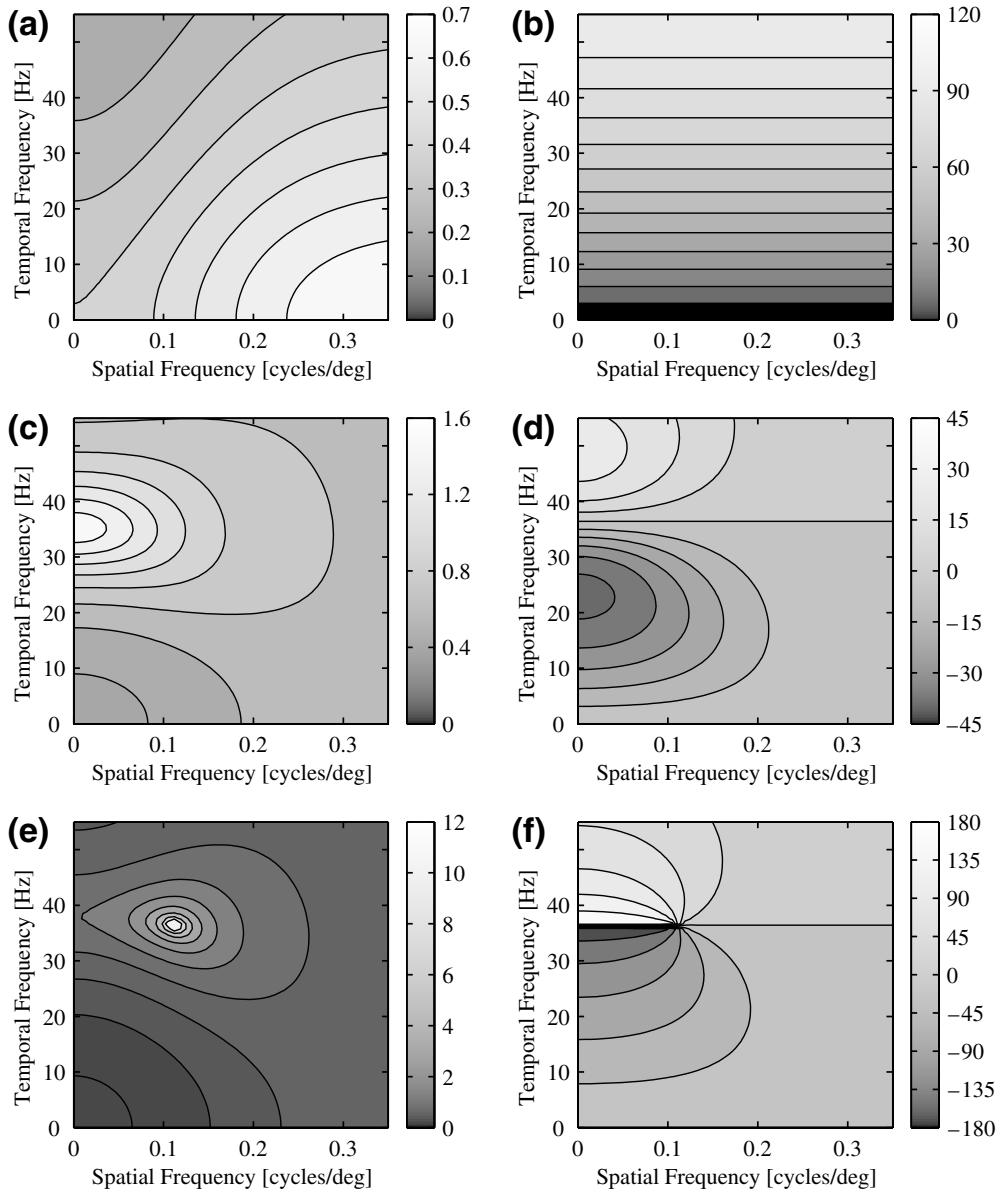


Figure 7. Retino-geniculate transfer ratio (left column) and phase shift (right column), as functions of both spatial and temporal grating frequencies. (a), (b) *Feedforward* model with continuous Gaussian inhibition, equation (44). Temporal parameters: $\Delta = 2$ ms, $\tau = 5$ ms; spatial parameters as in figure 1. The transfer ratio indicates low-pass temporal and high-pass spatial filtering, with increasing phase delay for higher temporal frequencies. (c), (d) *Feedback* model, equation (45). Temporal parameters: $\Delta = 10$ ms, $\tau = 5$ ms; spatial parameters as in figure 1. The feedback circuit has a preferred temporal frequency around 35 Hz, and is a spatial low-pass filter for these temporal frequencies, while operating as a spatial high-pass for lower temporal frequencies. Signals near the preferred frequency are transmitted without phase delay (horizontal contour line in (d)). (e), (f) Same as (c), (d), but with tripled inhibitory feedback strength, $D_{fb} = 2.43$. The transfer function now has a resonance at $\nu^* \approx 0.11$ cycles/deg, $f^* \approx 36.4$ Hz: the transfer ratio diverges, and the phase shift shows a pinwheel structure. Note that contour lines in (e) are spaced logarithmically for greater clarity, and that the colour axis is truncated.

One is thus left with

$$\tilde{T}_{\text{rg}}(\nu, f) = \frac{B_{\text{fb}}}{1 + D_{\text{fb}} e^{-\pi^2 \nu^2 d_{\text{fb}}^2} e^{i2\pi \Delta f} / (1 - i2\pi \tau f)}. \quad (45)$$

For zero temporal frequency, $f = 0$, these feedforward and feedback expressions reduce to the corresponding ‘spatial’ transfer ratio expressions in equations (34) and (41), respectively.

Figure 7 shows both the transfer ratio ($|\tilde{T}(\nu, f)|$) and the transfer phase shift ($\arg \tilde{T}(\nu, f)$) for feedforward and feedback cases, using the spatial parameters obtained from fitting the data by Cheng *et al* (1995). The best-fit curves from figure 1 thus correspond to the values along the x -axes ($f = 0$) in figures 7(a) and (c).

For the temporal coupling parameters we have set the time constant τ to 5 ms in both the feedforward and the feedback model. However, while we have chosen a short delay Δ of merely 2 ms for the feedforward case which involves monosynaptic and bisynaptic connections, we have chosen a longer delay of 10 ms for the feedback case which involves the thalamo-cortical loop.

As seen from figure 7, the spatiotemporal structure of the transfer ratios and phase shifts are quite different in the two cases (top and centre row), and this may imply that the relative role of the feedforward and feedback circuits may be distinguished by performing such experiments. Note that the purpose of showing these contour plots is merely to illustrate the potential of the method. The details should not be taken too seriously as, for example, the temporal parameters have been rather arbitrarily selected.

The bottom row of figure 7 indicates how the system would respond if inhibitory feedback were very strong (three times as strong as indicated by the fit to the Cheng *et al* data): the thalamo-cortical loop shows a resonance in this case, i.e. the system would respond most vigorously to a properly chosen grating. The conditions for the existence of a resonance, as well as the location of the latter, can be obtained as follows. A resonance occurs for ν - f -combinations for which the denominator in (45) vanishes. Solving for ν assuming that $D_{\text{fb}} > 0$, and requiring that ν must be a real number, one arrives at the following conditions:

$$\begin{aligned} 2\pi f \tau &\leq \sqrt{D_{\text{fb}}^2 - 1} \\ 2\pi f \Delta + \arctan 2\pi f \tau &= (2n + 1)\pi, \quad n \in \mathbb{Z}. \end{aligned} \quad (46)$$

If the first condition is fulfilled, and the latter equation has a real solution f^* , then the pertaining spatial frequency is given by

$$\nu^* = \frac{1}{\sqrt{2\pi} d_{\text{fb}}} \sqrt{\ln \frac{D_{\text{fb}}^2}{1 + 4\pi^2 f^{*2} \tau^2}}. \quad (47)$$

The existence of a singular point as seen in figures 7(e), (f) requires a transfer function which is not spatio-temporally separable. Clearly, if the spatial or temporal kernel diverges in a spatio-temporally separable transfer function, one would see a resonance ‘line’ in contour plots of the type shown in figure 7, not a resonance point.

5. Discussion

5.1. Linearity assumption

The modelling presented in this paper is based on *linear* theory. Thus, the feedforward coupling functions (coupling kernels) between retina and dLGN, and all the feedforward and feedback coupling functions between and within dLGN, TRN, and cortex illustrated in figure 5 are assumed to be linear. The feedback to relay cells from cortex and TRN will in general involve

nonlinear as well as linear effects (Sherman and Guillery 2001), whence we do not expect our approach to account for all behaviour of the retino-geniculate circuit. Instead it should be considered a linear, and thus readily analysable, entry point into mechanistic modelling of the geniculate circuit.

Given that the X pathway has been found to respond approximately linearly when driven by drifting-grating stimuli (So and Shapley 1981, Cheng *et al* 1995), our formalism should nevertheless be suitable for analysis of this pathway, at least under low-contrast conditions. It has further been demonstrated clearly that cortico-geniculate feedback affects the first-harmonic component of the relay cell response (Sillito and Jones 1997), indicating that the cortico-geniculate influence must have a significant linear component.

In *burst* mode (Sherman and Guillery 2001) the relay cells exhibit nonlinear behaviour due to low-threshold calcium spiking. Guido *et al* (1992) measured the linearity for a population of relay cells for lightly anesthetized cats both in their burst and tonic modes. In drifting-grating experiments the linear (first-harmonic) component was generally found to dominate the nonlinear (higher-order) components for cells in tonic mode, while the opposite was observed in burst mode. We thus expect our formalism to be best suited for cells in tonic mode, which appears to be the dominant mode in awake, attentive animals (Livingstone and Hubel 1981).

In other experiments the first-harmonic component of the X relay cell responses has been found to be much stronger than higher-order components, at least for low to moderate contrasts (So and Shapley 1981, Cheng *et al* 1995). This might indicate that the relay cells predominantly have been in tonic mode during their experiments.

We have developed this linear model with the X pathway in mind since this pathway exhibits rather linear response characteristics. Nonlinear characteristics of the Y pathway are already present at the retinal level, as demonstrated by large second-order Fourier components for Y retinal ganglion cells in drifting-grating experiments (Enroth-Cugell and Robson 1966, Hochstein and Shapley 1976). Note, however, that presence of second- or higher-order components in the relay cell responses (X or Y) does not in itself prove that the geniculate transfer function is nonlinear. Such higher-order components might in principle arise in the retina and be transferred linearly through dLGN. If so, it would be possible to measure the geniculate transfer function for each component separately and compare each component with the present linear expressions.

5.2. Assumption of spatial homogeneity

An assumption inherent throughout the mathematical analysis presented here is the assumption of spatial homogeneity, i.e. that all neurons at one level are alike except for the spatial location of their receptive field. This is expected to be a good approximation when the relevant neuronal populations are taken from a local region of the visual field. This criterion seems to be well satisfied by the feedforward coupling between retina and dLGN (Cleland *et al* 1971, Coenen and Vendrik 1972, Cleland and Lee 1985, Mastronarde 1987a, 1987b, 1992), while it is presently less certain for the connections involving TRN and cortex.

5.3. Feedback and spatio-temporal separability

Conflicting results have appeared in the literature on the question of spatio-temporal separability of the relay cell receptive field. Using sinusoidal grating patterns Enroth-Cugell *et al* (1983) and Dawis *et al* (1984) concluded that responses in cat retinal ganglion cells and dLGN relay cells are spatio-temporally coupled (i.e. not spatio-temporally separable) under these conditions. In white noise measurements DeAngelis *et al* (1995) and Wolfe and Palmer (1998) found relay cell receptive fields to be approximately separable.

Our theoretical work demonstrates that when feedback effects are present, the geniculate transfer function, and hence the relay cell spatiotemporal receptive field (inverse Fourier transform of $\tilde{G}_r(\mathbf{k}, \omega) = \tilde{T}_{rg}(\mathbf{k}, \omega)\tilde{G}_g(\mathbf{k}, \omega)$), cannot generally be spatio-temporally separable. For the relay cell spatiotemporal receptive field to be spatio-temporally separable, the Fourier transform $\tilde{G}_r(\mathbf{k}, \omega)$ must factor into a product $\tilde{G}_r^r(\mathbf{k})\tilde{G}_r^t(\omega)$, and this requires the same type of separation for $\tilde{G}_g(\mathbf{k}, \omega)$ and $\tilde{T}_{rg}(\mathbf{k}, \omega)$. With, for example, feedback inhibition on relay cells induced via cortical excitation of interneurons, the form of the geniculate transfer function \tilde{T}_{rg} in equation (35) shows $\tilde{T}_{rg}(\mathbf{k}, \omega) \neq \tilde{T}_{rg}^r(\mathbf{k})\tilde{T}_{rg}^t(\omega)$ in the general case. Only when the product $\tilde{h}_{ri}(\omega)\tilde{h}_{ic}(\omega)\tilde{h}_{cr}(\omega)$ can be approximated as a constant in equation (36) will spatio-temporal separation occur.

As seen from equation (30), this result generalizes to all circuits where feedback is involved: even if all coupling functions are spatio-temporally separable, the geniculate transfer function \tilde{T}_{rg} will not be separable. This result should be treated with a grain of salt, however: depending on stimulus properties and state of arousal, feedback may be very weak (e.g. cortical feedback upon presentation of spot stimuli), so that the denominator in equation (30) will be close to unity, possibly allowing for approximate spatio-temporal separation of the transfer ratio.

Note also that observations of spatio-temporal coupling in the relay cell receptive field do not necessarily imply that the geniculate transfer function is spatio-temporally coupled. A spatio-temporally separable geniculate transfer function would, in conjunction with a spatio-temporally coupled receptive field of retinal ganglion cells, result in a spatio-temporally coupled relay cell receptive field as well.

As illustrated for our example feedback model in figures 7(e) and (f), the existence of resonances in the geniculate transfer function for particular combinations of spatial and temporal frequencies would be a clear sign of spatio-temporal coupling.

5.4. ON-OFF mixing and luminance dependence

For the purely feedforward case, i.e. feedback from TRN and cortex neglected, the transfer function is found to be independent of both the mean luminance L_0 and the shape of the activity function $l(L_0)$. Due to the mixing of the ON and OFF channels at the reticular level, feedback from TRN will break this independence. The dependence on L_0 and $l(L_0)$ is specifically included in equation (30) via the term $\tilde{K}_{tr}^*(\mathbf{k}, \omega; L_0) \equiv \tilde{K}_{tr}(\mathbf{k}, \omega)[1 - c_1(L_0)]$. Similarly, cortical feedback is expected to break the mean-luminance independence of the transfer ratio, even though an expression for how the transfer ratio in this case depends on the mean luminance is not given in equation (30). We have not found any experimental data on the mean-luminance dependence of the retino-geniculate transfer ratio in the literature.

The linear transfer function expression in equation (30) can be extended to include other synaptic connections. For example, Singer and Creutzfeldt (1970) proposed mixing of ON-centre and OFF-centre relay cell inputs from retinal ganglion cells. As for the ON-OFF mixing at the reticular level considered here, this would also lead to transfer functions depending on the mean luminance L_0 . Another synaptic connection not considered here is an inhibitory influence on interneurons from reticular cells (Ahlsén *et al* 1985).

5.5. Contrast gain and contrast sensitivity

With the ganglion-cell response available one can also straightforwardly obtain the relay cell contrast gain (essentially $|\tilde{G}_r(\mathbf{k}, \omega)|$ (Watson 1992)) from the geniculate transfer function $\tilde{T}_{rg}(\mathbf{k}, \omega)$, i.e. $\tilde{G}_r(\mathbf{k}, \omega) = \tilde{T}_{rg}(\mathbf{k}, \omega)\tilde{G}_g(\mathbf{k}, \omega)$ (equation (18)). Moreover, the relay cell spatiotemporal impulse response function (essentially the receptive field) can be obtained by performing the inverse Fourier transform on $\tilde{G}_r(\mathbf{k}, \omega)$.

The so-called *contrast sensitivity* is a measure of the ability to distinguish signal from noise, and Watson (1990) has provided an expression, applicable to individual (linear) neurons, relating contrast sensitivity, contrast gain and noise spectrum. This connection is needed if one hopes to link neuron modelling to psychophysical observations. Watson (1992) also showed how to relate contrast sensitivities at different levels in the visual system, and applied the formalism to relate the sensitivities of parvocellular dLGN neurons and cortical cells in the primate. But Watson's mathematical model for the geniculate transfer functions was purely *descriptive*, while the goal of this work is to contribute to the development of *mechanistic* models based on the known neuronal circuitry.

5.6. Significance

We consider the establishment of the general mathematical expression for the geniculate transfer function $\tilde{T}_{\text{rg}}(\mathbf{k}, \omega)$, equation (30), for the full geniculate circuit shown in figures 3 and 5, to be the most important result in this paper. The other transfer function expressions in equations (18), (23), (28), and (29) can straightforwardly be obtained by omitting terms in the extended-circuit expression. The expression is based on linear theory and is thus applicable only for the linear regime, i.e. for small to medium grating contrasts.

The general formula equation (30) allows, in conjunction with the appropriate drifting-grating data, for rigorous testing of candidate models for the retino-geniculate circuit. Any mechanistic model which claims to account for the behaviour of the retino-geniculate circuit must provide correct predictions for the linear regime. The mechanistic models are represented by the choices of coupling functions $K_{mn}(\mathbf{r}, t)$. The drifting-grating experimental data must include both the relay cell output (action potentials) and the retinal input (S-potentials) and should be recorded under conditions where the response is as linear as possible, i.e. low grating contrast. Preferably, the transfer ratio (and phase shift) should be measured for a set of combinations of spatial and temporal grating frequencies, i.e. a grid of points in the ν - f -plane. Experimental recordings at different mean luminances L_0 would also be desirable.

We demonstrated how mechanistic models could be tested against experiments by considering the data of Cheng *et al* (1995) and exploring two specific example models. The main purpose of this demonstration was to illustrate the practical use of the method. This data set is quite limited (only a single temporal frequency). Further, it was recorded with a significant grating contrast (32%), presumably too high to be in a clearly linear regime.

The good, but not perfect, fits of the purely feedforward (equation (34)) and purely feedback (equation (41)) models to the example data set observed in figure 1(b) could certainly be improved by considering more complex models. For example, one could consider a model with *both* feedforward and feedback coupling. This would, however, add more fitting parameters to the procedure and probably lead to over-fitting of the rather limited example data set.

A consequence of the feedback pathways from TRN and cortex is that the theoretical expression for the retino-geniculate transfer ratio may diverge for particular combinations of spatial and temporal frequencies. A model example of this phenomenon is given in figure 7(e). In the experimental situation this would correspond to a resonance peak in the ν - f -plane. Whether such a resonance peak can occur under typical experimental conditions is an open question since the phenomenon depends on an appropriate combination of circuit parameters.

The cortical cells have been lumped into a single cortical neuronal population in our modelling approach (see section 3.2.4), and the response properties of this neuronal population are described in a descriptive manner. This does not, however, in itself preclude that intracortical processing may be accounted for in our modelling scheme; linear cortical processing may be included by choosing the coupling kernel K_{cr} appropriately.

Recently, Kirkland and Gerstein (1998) and Kirkland *et al* (2000) have modelled the cortico-geniculate system to explore cortically induced synchronization and long-term correlations of dLGN relay cells. The study of synchronization of spikes between neurons by its very nature requires spiking neuron models, but these are usually not amenable to mathematical analysis and thus require large-scale computer simulations. In interpreting the results of such simulations, one often faces similar problems as when interpreting experimental data, such as scarcity of data (due to limited computer time), or sampling bias. We therefore believe that firing-rate models as presented here are preferable to spiking neuron models whenever applicable, because they allow for deeper mathematical analysis and typically require only numerical evaluation, but not randomized simulation, and thus yield more readily interpretable results.

A good approach to investigate models for the geniculate circuitry would be to record the response of individual neurons to different kinds of visual stimuli. Then a mathematical model fitted to experimental results for one type of stimuli would make testable predictions for experiments with another type of stimuli. Such testing would increase the constraints on the mathematical modelling and make it easier to falsify a proposed general quantitative model for the signal processing in dLGN. An example of such an approach used on the *limulus* retina is given by Brodie *et al* (1978a, 1978b).

In such a scheme one needs to relate the quantities measured in the different types of experiments. Einevoll and Heggelund (2000) derived expressions for the spatial receptive field for dLGN relay cells (and intrageniculate interneurons) for several mechanistic models for feedforward inhibition at the geniculate level. They further derived expressions for the corresponding responses to flashing circular light (or dark) spot stimuli to allow for a comparison with recent experimental data from Ruksenas *et al* (2000). In Einevoll *et al* (2000) we derived the connection between these purely spatial receptive fields and the spatiotemporal impulse–response function measured in experiments using drifting gratings (or white noise analysis). Here we have derived general expressions for the geniculate transfer function measured in drifting-grating experiments and have shown with examples how specific models can be tested against experimental data. Thus the mathematical formalism now exists for testing mechanistic models for retino-geniculate circuitry against both flashing-spot (and flashing-bar) and drifting-grating experiments. Experiments on relay cells driven by different types of stimuli during a single recording would thus significantly constrain the possible mechanistic models for the organization of the geniculate circuitry.

Acknowledgments

HEP was supported by a Marie Curie Fellowship of the European Union. We thank Paul Heggelund and Klaus Funke for critical reading of the manuscript.

Appendix A

In this appendix we derive the expression for the geniculate transfer ratio for X-ON cells when feedback from TRN is included.

The descriptive expression for a TRN cell to drifting gratings is in analogy with equation (14), given as

$$R_t(\mathbf{r}, t) = l_{\text{ON}}(L_0)\tilde{G}_t(\mathbf{0}, 0) + L_0 l'_{\text{ON}}(L_0)m\tilde{G}_t(\mathbf{k}, \omega)e^{i(\mathbf{k}\mathbf{r} - \omega t)}. \quad (\text{A.1})$$

In analogy with equation (15) we also have

$$R_t(\mathbf{r}, t) = \int_{\tau} \iint_{r_0} [K_{\text{tr}}^{\text{ON}}(\mathbf{r} - \mathbf{r}_0, \tau)R_{\text{r}}^{\text{ON}}(\mathbf{r}_0, t - \tau) + K_{\text{tr}}^{\text{OFF}}(\mathbf{r} - \mathbf{r}_0, \tau)R_{\text{r}}^{\text{OFF}}(\mathbf{r}_0, t - \tau) + K_{\text{tt}}(\mathbf{r} - \mathbf{r}_0, \tau)R_t(\mathbf{r}_0, t - \tau)] d^2r_0 d\tau. \quad (\text{A.2})$$

Here $K_{tr}^{ON}(r - r_0, \tau)(K_{tr}^{OFF}(r - r_0, \tau))$ is the spatio-temporal coupling function describing the excitatory influence of a relay ON-cell (OFF-cell) on a TRN cell, and $K_{tt}(r - r_0, \tau)$ is correspondingly describing the coupling function between two TRN cells. In analogy to the derivation in equation (16) we find

$$\begin{aligned} R_t(r, t) &= l_{ON}(L_0)[\tilde{K}_{tr}^{ON}(\mathbf{0}, 0)\tilde{G}_r^{ON}(\mathbf{0}, 0) + c_0(L_0)\tilde{K}_{tr}^{OFF}(\mathbf{0}, 0)\tilde{G}_r^{OFF}(\mathbf{0}, 0) \\ &\quad + \tilde{K}_{tt}(\mathbf{0}, 0)\tilde{G}_t(\mathbf{0}, 0)] + mL_0l'_{ON}(L_0)\left[\tilde{K}_{tr}^{ON}(\mathbf{k}, \omega)\tilde{G}_r^{ON}(\mathbf{k}, \omega) \right. \\ &\quad \left. - c_1(L_0)\tilde{K}_{tr}^{OFF}(\mathbf{k}, \omega)\tilde{G}_r^{OFF}(\mathbf{k}, \omega) + \tilde{K}_{tt}(\mathbf{k}, \omega)\tilde{G}_t(\mathbf{k}, \omega)\right]e^{i(kr-\omega t)} \\ &= l_{ON}(L_0)\tilde{G}_t(\mathbf{0}, 0) + mL_0l'_{ON}(L_0)\tilde{G}_t(\mathbf{k}, \omega)e^{i(kr-\omega t)}, \end{aligned} \quad (A.3)$$

where we have introduced the functions

$$c_0(L_0) \equiv l_{OFF}(L_0)/l_{ON}(L_0), \quad c_1(L_0) \equiv -l'_{OFF}(L_0)/l'_{ON}(L_0), \quad (A.4)$$

and used equation (A.1) in the last step.

We now make the assumption that the ON- and OFF-channels are identical except for the difference in the functions $l_{OFF}(L_0)$ and $l_{ON}(L_0)$. Mathematically this corresponds to $\tilde{K}_{tr}^{ON}(\mathbf{k}, \omega) = \tilde{K}_{tr}^{OFF}(\mathbf{k}, \omega) \equiv \tilde{K}_{tr}(\mathbf{k}, \omega)$ and $\tilde{G}_r^{ON}(\mathbf{k}, \omega) = \tilde{G}_r^{OFF}(\mathbf{k}, \omega) \equiv \tilde{G}_r(\mathbf{k}, \omega)$.

Then we identify

$$\begin{aligned} \tilde{G}_t(\mathbf{0}, 0) &= \frac{\tilde{K}_{tr}(\mathbf{0}, 0)\tilde{G}_r(\mathbf{0}, 0)[1 + c_0(L_0)]}{1 - \tilde{K}_{tt}(\mathbf{0}, 0)}, \\ \tilde{G}_t(\mathbf{k}, \omega) &= \frac{\tilde{K}_{tr}(\mathbf{k}, \omega)\tilde{G}_r(\mathbf{k}, \omega)[1 - c_1(L_0)]}{1 - \tilde{K}_{tt}(\mathbf{k}, \omega)}, \quad [\mathbf{k}, \omega] \neq [\mathbf{0}, 0]. \end{aligned} \quad (A.5)$$

The response of an X-ON relay cell to a drifting grating is then given as

$$\begin{aligned} R_r^{ON}(r, t) &= \int_{\tau} \iint_{r_0} [K_{rg}(r - r_0, \tau)R_g^{ON}(r_0, t - \tau) + K_{ri}(r - r_0, \tau)R_i^{ON}(r_0, t - \tau) \\ &\quad + K_{rt}(r - r_0, \tau)R_t(r_0, t - \tau)] d^2r_0 d\tau \\ &= l_{ON}(L_0)[\tilde{K}_{rg}(\mathbf{0}, 0)\tilde{G}_g(\mathbf{0}, 0) + \tilde{K}_{ri}(\mathbf{0}, 0)\tilde{G}_i(\mathbf{0}, 0) \\ &\quad + \tilde{K}_{rt}(\mathbf{0}, 0)\tilde{G}_t(\mathbf{0}, 0)] + L_0l'_{ON}(L_0)m[\tilde{K}_{rg}(\mathbf{k}, \omega)\tilde{G}_g(\mathbf{k}, \omega) \\ &\quad + \tilde{K}_{ri}(\mathbf{k}, \omega)\tilde{G}_i(\mathbf{k}, \omega) + \tilde{K}_{rt}(\mathbf{k}, \omega)\tilde{G}_t(\mathbf{k}, \omega)]e^{i(kr-\omega t)} \\ &= l_{ON}(L_0)\left[\tilde{K}_{rg}(\mathbf{0}, 0) + \tilde{K}_{ri}(\mathbf{0}, 0)\tilde{K}_{ig}(\mathbf{0}, 0)\right]\tilde{G}_g(\mathbf{0}, 0) \\ &\quad + \frac{\tilde{K}_{rt}(\mathbf{0}, 0)\tilde{K}_{tr}(\mathbf{0}, 0)[1 + c_0(L_0)]}{1 - \tilde{K}_{tt}(\mathbf{0}, 0)}\tilde{G}_r(\mathbf{0}, 0) \\ &\quad + L_0l'_{ON}(L_0)m\left[\tilde{K}_{rg}(\mathbf{k}, \omega) + \tilde{K}_{ri}(\mathbf{k}, \omega)\tilde{K}_{ig}(\mathbf{k}, \omega)\right]\tilde{G}_g(\mathbf{k}, \omega) \\ &\quad + \frac{\tilde{K}_{rt}(\mathbf{k}, \omega)\tilde{K}_{tr}(\mathbf{k}, \omega)[1 - c_1(L_0)]}{1 - \tilde{K}_{tt}(\mathbf{k}, \omega)}\tilde{G}_r(\mathbf{k}, \omega)\right]e^{i(kr-\omega t)} \\ &= l_{ON}(L_0)\tilde{G}_r(\mathbf{0}, 0) + L_0l'_{ON}(L_0)m\tilde{G}_r(\mathbf{k}, \omega)e^{i(kr-\omega t)}, \end{aligned} \quad (A.6)$$

where we have used equations (14), (A.1), and (A.5).

By term-wise comparison of the last two equations in equation (A.6) we can as before determine $\tilde{G}_r(\mathbf{0}, 0)$ and $\tilde{G}_r(\mathbf{k}, \omega)$. The transfer function of the *modulated* response is now given by equation (28) in the main text. Correspondingly, the transfer ratio for the *mean* response is given by equation (29).

Appendix B

This appendix shows the derivation of the geniculate transfer function $\tilde{T}_{\text{rg}}(\mathbf{k}, \omega)$ when the complete geniculate circuit in figure 5 is considered.

With feedforward excitation for retinal ganglion cells, feedforward inhibition from intrageniculate interneurons, feedback inhibition from TRN cells, and feedback excitation from cortex, the response for a relay cell is given by

$$R_{\text{r}}(\mathbf{r}, t) = \int_{\tau} \iint_{r_0} [K_{\text{rg}}(\mathbf{r} - \mathbf{r}_0, \tau) R_{\text{g}}(\mathbf{r}_0, t - \tau) + K_{\text{ri}}(\mathbf{r} - \mathbf{r}_0, \tau) R_{\text{i}}(\mathbf{r}_0, t - \tau) + K_{\text{rt}}(\mathbf{r} - \mathbf{r}_0, \tau) R_{\text{t}}(\mathbf{r}_0, t - \tau) + K_{\text{rc}}(\mathbf{r} - \mathbf{r}_0, \tau) R_{\text{c}}(\mathbf{r}_0, t - \tau)] d^2 r_0 d\tau. \quad (\text{B.1})$$

In analogy to the derivation in equation (16) we find

$$\begin{aligned} R_{\text{r}}(\mathbf{r}, t) &= l(L_0) [\tilde{K}_{\text{rg}}(\mathbf{0}, 0) \tilde{G}_{\text{g}}(\mathbf{0}, 0) + \tilde{K}_{\text{ri}}(\mathbf{0}, 0) \tilde{G}_{\text{i}}(\mathbf{0}, 0) \\ &\quad + \tilde{K}_{\text{rt}}(\mathbf{0}, 0) \tilde{G}_{\text{t}}(\mathbf{0}, 0) + \tilde{K}_{\text{rc}}(\mathbf{0}, 0) \tilde{G}_{\text{c}}(\mathbf{0}, 0)] \\ &\quad + L_0 l'(L_0) m [\tilde{K}_{\text{rg}}(\mathbf{k}, \omega) \tilde{G}_{\text{g}}(\mathbf{k}, \omega) + \tilde{K}_{\text{ri}}(\mathbf{k}, \omega) \tilde{G}_{\text{i}}(\mathbf{k}, \omega) \\ &\quad + \tilde{K}_{\text{rt}}(\mathbf{k}, \omega) \tilde{G}_{\text{t}}(\mathbf{k}, \omega) + \tilde{K}_{\text{rc}}(\mathbf{k}, \omega) \tilde{G}_{\text{c}}(\mathbf{k}, \omega)] e^{i(\mathbf{k}\mathbf{r} - \omega t)} \\ &= l(L_0) \tilde{G}_{\text{r}}(\mathbf{0}, 0) + L_0 l'(L_0) m \tilde{G}_{\text{r}}(\mathbf{k}, \omega) e^{i(\mathbf{k}\mathbf{r} - \omega t)}, \end{aligned} \quad (\text{B.2})$$

and we identify

$$\begin{aligned} \tilde{G}_{\text{r}}(\mathbf{k}, \omega) &= \tilde{K}_{\text{rg}}(\mathbf{k}, \omega) \tilde{G}_{\text{g}}(\mathbf{k}, \omega) \\ &\quad + \tilde{K}_{\text{ri}}(\mathbf{k}, \omega) \tilde{G}_{\text{i}}(\mathbf{k}, \omega) + \tilde{K}_{\text{rt}}(\mathbf{k}, \omega) \tilde{G}_{\text{t}}(\mathbf{k}, \omega) + \tilde{K}_{\text{rc}}(\mathbf{k}, \omega) \tilde{G}_{\text{c}}(\mathbf{k}, \omega). \end{aligned} \quad (\text{B.3})$$

Likewise we find

$$\begin{aligned} \tilde{G}_{\text{i}}(\mathbf{k}, \omega) &= \tilde{K}_{\text{ig}}(\mathbf{k}, \omega) \tilde{G}_{\text{g}}(\mathbf{k}, \omega) + \tilde{K}_{\text{ic}}(\mathbf{k}, \omega) \tilde{G}_{\text{c}}(\mathbf{k}, \omega), \\ \tilde{G}_{\text{t}}(\mathbf{k}, \omega) &= \tilde{K}_{\text{tr}}(\mathbf{k}, \omega) [1 - c_1(L_0)] \tilde{G}_{\text{r}}(\mathbf{k}, \omega) + \tilde{K}_{\text{tt}}(\mathbf{k}, \omega) \tilde{G}_{\text{t}}(\mathbf{k}, \omega) + \tilde{K}_{\text{tc}}(\mathbf{k}, \omega) \tilde{G}_{\text{c}}(\mathbf{k}, \omega), \\ \tilde{G}_{\text{c}}(\mathbf{k}, \omega) &= \tilde{K}_{\text{cr}}(\mathbf{k}, \omega) \tilde{G}_{\text{r}}(\mathbf{k}, \omega). \end{aligned} \quad (\text{B.4})$$

Equations (B.3) and (B.4) represent four equations for $\tilde{G}_{\text{r}}(\mathbf{k}, \omega)$, $\tilde{G}_{\text{i}}(\mathbf{k}, \omega)$, $\tilde{G}_{\text{t}}(\mathbf{k}, \omega)$, and $\tilde{G}_{\text{c}}(\mathbf{k}, \omega)$, which when solved give

$$\begin{aligned} \tilde{G}_{\text{r}}(\mathbf{k}, \omega) &= \\ &= \frac{[\tilde{K}_{\text{rg}}(\mathbf{k}, \omega) + \tilde{K}_{\text{ri}}(\mathbf{k}, \omega) \tilde{K}_{\text{ig}}(\mathbf{k}, \omega)] \tilde{G}_{\text{g}}(\mathbf{k}, \omega)}{1 - \tilde{K}_{\text{rc}}(\mathbf{k}, \omega) \tilde{K}_{\text{cr}}(\mathbf{k}, \omega) - \tilde{K}_{\text{ri}}(\mathbf{k}, \omega) \tilde{K}_{\text{ic}}(\mathbf{k}, \omega) \tilde{K}_{\text{cr}}(\mathbf{k}, \omega) - \frac{\tilde{K}_{\text{ri}}(\mathbf{k}, \omega) \tilde{K}_{\text{tr}}^*(\mathbf{k}, \omega) + \tilde{K}_{\text{rt}}(\mathbf{k}, \omega) \tilde{K}_{\text{tc}}(\mathbf{k}, \omega) \tilde{K}_{\text{cr}}(\mathbf{k}, \omega)}{1 - \tilde{K}_{\text{tt}}(\mathbf{k}, \omega)}}} \end{aligned} \quad (\text{B.5})$$

Here we have introduced the shorthand notation $\tilde{K}_{\text{tr}}^*(\mathbf{k}, \omega) \equiv \tilde{K}_{\text{tr}}(\mathbf{k}, \omega) [1 - c_1(L_0)]$. The geniculate transfer function in equation (30) then follows immediately.

References

- Ahlsén G, Lindström S and Lo F-S 1983 Excitation of perigeniculate neurones from X and Y principal cells in the lateral geniculate nucleus of the cat *Acta Physiol. Scand.* **118** 445–8
- Ahlsén G, Lindström S and Lo F-S 1985 Interaction between inhibitory pathways to principal cells in the lateral geniculate nucleus of the cat *Exp. Brain Res.* **58** 134–43
- Bishop P O, Burke W and Davis R 1958 Synapse discharge by single fibre in mammalian visual system *Nature* **182** 728–30
- Brodie S E, Knight B W and Ratliff F 1978a The response of the *limulus* retina to moving stimuli: a prediction by Fourier synthesis *J. Gen. Physiol.* **72** 129–66

- Brodie S E, Knight B W and Ratliff F 1978b The spatiotemporal transfer function of the *limulus* lateral eye *J. Gen. Physiol.* **72** 167–202
- Cheng H, Chino Y M, Smith E L, Hamamoto J and Yoshida K 1995 Transfer characteristics of lateral geniculate nucleus X neurons in the cat: effects of spatial frequency and contrast *J. Neurophysiol.* **74** 2548–57
- Cleland B G, Dubin M W and Levick W R 1971 Sustained and transient neurones in cat's retina and lateral geniculate nucleus *J. Physiol.* **217** 473–96
- Cleland B G and Lee B B 1985 A comparison of visual responses of cat lateral geniculate nucleus neurones with those of ganglion cells afferent to them *J. Physiol.* **369** 249–68
- Coenen A M L and Vendrik A J H 1972 Determination of the transfer ratio of cat's geniculate neurons through quasi-intracellular recordings and the relation with the level of alertness *Exp. Brain Res.* **14** 227–42
- Dawis S, Shapley R, Kaplan E and Tranchina D 1984 The receptive field organization of X-cells in the cat: Spatiotemporal coupling and asymmetry *Vis. Res.* **24** 549–64
- Dayan P and Abbott L F 2001 *Theoretical Neuroscience* (Cambridge, MA: MIT Press)
- DeAngelis G, Ohzawa I and Freeman R 1995 Receptive field dynamics in the central visual pathways *Trends Neurosci.* **18** 451–8
- Dubin M W and Cleland B G 1977 Organization of visual inputs to interneurons of lateral geniculate nucleus of cat *J. Neurophysiol.* **40** 410–27
- Einevoll G T, Kocbach A and Heggelund P 2000 Probing the retino-geniculate circuit in cat using circular spot stimuli *Neurocomputing* **32–33** 727–33
- Einevoll G T and Heggelund P 2000 Mathematical models for the spatial receptive-field organization of nonlagged X cells in dorsal lateral geniculate nucleus of cat *Vis. Neurosci.* **17** 871–86
- Enroth-Cugell C and Robson J G 1966 The contrast sensitivity of retinal ganglion cells of the cat *J. Physiol.* **187** 517–52
- Enroth-Cugell C, Robson J G, Schweitzer-Tong D E and Watson A B 1983 Spatio-temporal interactions in cat retinal ganglion cells showing linear spatial summation *J. Physiol.* **341** 279–307
- Funke K and Eysel U 1998 Inverse correlation of firing patterns of single topographically matched perigeniculate neurons and cat dorsal lateral geniculate relay cells *Vis. Neurosci.* **15** 711–29
- Guido W, Lu S-M and Sherman S M 1992 Relative contributions of burst and tonic responses to the receptive field properties of lateral geniculate neurons in the cat *J. Neurophysiol.* **68** 2199–211
- Heeger D J 1991 Nonlinear model of neural responses in cat visual cortex *Computational Models of Visual Processing* ed M S Landy and J A Movshon (Cambridge, MA: MIT Press) pp 119–34
- Hochstein S and Shapley R M 1976 Quantitative analysis of retinal ganglion cell classifications *J. Physiol.* **262** 237–64
- Hubel D and Wiesel T N 1961 Integrative action in the cat's lateral geniculate body *J. Physiol.* **155** 385–98
- Kaplan E, Marcus S and So Y T 1979 Effects of dark adaptation on spatial and temporal properties of receptive fields in cat lateral geniculate nucleus *J. Physiol.* **294** 561–80
- Kaplan E and Shapley R M 1984 The origin of the S (slow) potential in the mammalian lateral geniculate nucleus *Exp. Brain Res.* **55** 111–16
- Kirkland K L and Gerstein G L 1998 A model of cortically induced synchronization in the lateral geniculate nucleus of the cat: a role for low-threshold calcium channels *Vis. Res.* **38** 2007–22
- Kirkland K L, Sillito A M, Jones H E, West D C and Gerstein G L 2000 Oscillations and long-lasting correlations in a model of the lateral geniculate nucleus and visual cortex *J. Neurophysiol.* **84** 1863–8
- Kocbach A, Einevoll G T and Heggelund P 2001 Probing mechanistic models for the retinogeniculate circuit in cat using drifting gratings *Neurocomputing* **38–40** 727–32
- Leibovic K N 1990 Vertebrate photoreceptors *Science of Vision* ed K N Leibovic (New York: Springer) pp 16–52
- Lindström S and Wróbel A 1990 Private inhibitory systems for the X and Y pathways in the dorsal lateral geniculate nucleus of the cat *J. Physiol.* **429** 259–80
- Livingstone M S and Hubel D H 1981 Effects of sleep and arousal on the processing of visual information in the cat *Nature* **291** 554–61
- Lo F S and Sherman S M 1994 Feedback inhibition in the cat's lateral geniculate nucleus *Exp. Brain Res.* **100** 365–8
- Marmarelis P Z and Marmarelis V Z 1977 *Analysis of Physiological Systems* (New York: Plenum)
- Mastrorarde D N 1987a Two classes of single-input X-cells in cat lateral geniculate nucleus. I. Receptive-field properties and classification of cells *J. Neurophysiol.* **57** 357–80
- Mastrorarde D N 1987b Two classes of single-input X-cells in cat lateral geniculate nucleus. II. Retinal inputs and the generation of receptive-field properties *J. Neurophysiol.* **57** 381–413
- Mastrorarde D N 1992 Non-lagged relay cells and interneurons in the cat lateral geniculate nucleus: receptive field properties and retinal inputs *Vis. Neurosci.* **8** 407–41
- McCormick D 1992 Neurotransmitter actions in the thalamus and cerebral cortex and their role in neuromodulation of thalamocortical activity *Prog. Neurobiol.* **39** 337–88

- Mukherjee P and Kaplan E 1995 Dynamics of neurons in the cat lateral geniculate nucleus: in vivo electrophysiology and computational modelling *J. Neurophysiol.* **74** 1222–43
- Murphy P C, Duckett S G and Sillito A M 1999 Feedback connections to the lateral geniculate nucleus and cortical response properties *Science* **286** 1552–4
- Norton T T, Holdefer R N and Godwin D W 1989 Effects of bicuculline on receptive field center sensitivity of relay cells in lateral geniculate nucleus *Brain Res.* **488** 348–52
- Oppenheim A F and Willsky A S 1997 *Signals and Systems* 2nd edn (Upper Saddle River, NJ: Prentice-Hall)
- Peichl L and Wässle H 1979 Size, scatter and coverage of ganglion cell receptive field centres in the cat retina *J. Physiol.* **291** 117–41
- Rodieck R W 1965 Quantitative analysis of cat retinal ganglion cell response to visual stimuli *Vis. Res.* **5** 583–601
- Ruksenas O, Fjeld I T and Heggelund P 2000 Spatial summation and center-surround antagonism in the receptive field of single units in the dorsal lateral geniculate nucleus of cat: Comparison with retinal input *Vis. Neurosci.* **17** 855–70
- Shapley R and Lennie P 1985 Spatial frequency analysis in the visual system *Ann. Rev. Neurosci.* **8** 547–83
- Sherman S M and Guillery R W 1996 Functional organization of thalamocortical relays *J. Neurophysiol.* **76** 1367–95
- Sherman S M and Guillery R W 2001 *Exploring the Thalamus* (New York: Academic)
- Sillito A M, Cudeiro J and Murphy P C 1993 Orientation sensitive elements in the corticofugal influence on centre-surround interactions in the dorsal lateral geniculate nucleus *Exp. Brain Res.* **93** 6–16
- Sillito A M and Jones H E 1997 Functional organization influencing neurotransmission in the lateral geniculate nucleus *Thalamus* vol 2, ed M Steriade, E G Jones and D A McCormick (New York: Elsevier) pp 1–52
- Singer W and Creutzfeldt O D 1970 Reciprocal inhibition of ON- and OFF-center neurones in the lateral geniculate body of the cat *Exp. Brain Res.* **10** 311–30
- So Y T and Shapley R 1981 Spatial tuning of cells in and around lateral geniculate nucleus of the cat: X and Y relay cells and perigeniculate interneurons *J. Neurophysiol.* **45** 107–20
- Steriade M, Jones E G and McCormick D A 1997 *Thalamus* (New York: Elsevier)
- Uhlrich D J, Tamamaki N, Murphy P C and Sherman S M 1995 Effects of brain stem parabrachial activation on receptive field properties of cells in the cat's lateral geniculate nucleus *J. Neurophysiol.* **73** 2428–47
- Watson A B 1990 Gain, noise, and contrast sensitivity of linear visual neurons *Vis. Neurosci.* **4** 147–57
- Watson A B 1992 Transfer of contrast sensitivity in linear visual networks *Vis. Neurosci.* **8** 65–76
- Wolfe J and Palmer L A 1998 Temporal diversity in the lateral geniculate nucleus of cat *Vis. Neurosci.* **15** 653–75